Design, Development, and Field-Testing of a Cost-Optimized Village-Scale, Photovoltaic-Powered, Electrodialysis Reversal Water Desalination System for Rural India

by

David W. Bian

S.B. Mechanical Engineering
Massachusetts Institute of Technology (2015)

Submitted to the Department of Mechanical Engineering
in partial fulfillment of the requirements for the degree of

Master of Science in Mechanical Engineering

at the

MASSACHUSETTS INSTITUTE OF TECHNOLOGY

June 2017

Author ..... Signature redacted
Department of Mechanical Engineering
May 12, 2017

Certified by ..... Signature redacted
Amos G. Winter, V.
Assistant Professor of Mechanical Engineering
Thesis Supervisor

Accepted by ..... Signature redacted
Rohan Abeyaratne
Professor of Mechanical Engineering
Chairman, Committee on Graduate Students

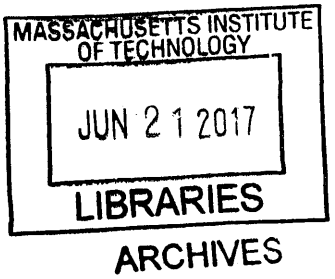

Design, Development, and Field-Testing of a Cost-Optimized Village-Scale, Photovoltaic-Powered, Electrodialysis Reversal Water Desalination System for Rural India

by

David W. Bian

Submitted to the Department of Mechanical Engineering
on May 12, 2017, in partial fulfillment of the requirements for the
degree of Master of Science in Mechanical Engineering

Abstract

The aim of this research was to identify the effectiveness of cost-optimizing a photovoltaic-powered electrodialysis reversal (PV-EDR) system for village-scale applications in rural India based on current component costs and performance. Currently available village-scale off-grid desalination systems have high capital costs – $11,250 USD compared to $4,500 USD for equivalent grid-connected systems – rendering them prohibitively expensive for cost-constrained communities. Compared to current state-of-the-art PV-powered reverse osmosis desalination systems, electrodialysis has the potential to reduce capital cost due to the lower energy requirement of the ED process at brackish feed water salinities.

The parametric relationships that govern the characteristics of the electrodialysis process and photovoltaic power systems were investigated and a model was created to predict a PV-EDR system's cost and performance. Through optimization, it was found that the optimal design was composed of a GE Water electrodialysis stack with 62 cell pairs, an applied stack voltage of 45 V, a batch size of 0.42 m^3, and a power system with 57.5 m^2 of photovoltaic solar panels and 22 kWh of batteries. The system is predicted to run 17.7 hours per day on average and cost $23,420. This was a 42% reduction from the $40,138 cost of a PV-EDR system designed using the conventional engineering practice of sequentially designing the load and then the power system.

A sensitivity analysis was conducted to evaluate the effects of different parameter changes on optimal system cost and design. The analysis revealed that relaxing the reliability requirement from 100% to 98% would reduce the optimal cost by 5.7%. An ED membrane cost reduction of 87% would cause the previous optimal system design to have a system cost of $15,360. The analysis revealed that optimizing the system with the lower membrane cost results in a system with a different configuration and a system cost of $11,717, a 24% additional cost reduction that was enabled by a flexible operation schedule since the lower membrane cost optimized system would operate on average for 8.6 hours per day instead of 17.7.

A pilot PV-EDR system was built and installed in the village of Chelluru in

India, where a week-long trial was conducted to collect initial data and results. With the exception of a few practicalities not considered in the model, the experimental results closely matched the PV-EDR system performance model on the basis of solar irradiance, batch power and battery energy levels. To fully validate the model and make it more accurate, long-term field testing must be conducted over the course of a full annual irradiance cycle.

Thesis Supervisor: Amos G. Winter, V.
Title: Assistant Professor of Mechanical Engineering

Acknowledgments

While this thesis focuses on my work and contributions, none of this would have been possible without the help and support of amazing advisors, researchers, engineers, friends and sponsors.

I would like to thank the following people:

- First and foremost, my advisor, **Professor Amos Winter**, the principal investigator of the Global Engineering and Research (GEAR) Lab. It had always been a dream of mine to work at the intersection of engineering and global development, and even today I am still humbled that he accepted me into his exceptional research group. It has truly been an honor to have the opportunity to work with him on such a cool project as village-scale desalination. He has always been upfront about and understanding of my many mistakes, and through his guidance, I feel that I have become both a better engineer and communicator. If I one day become half the teacher, half the engineer, half the inspiration that Amos is, I will consider it one of my greatest accomplishments.

- **Sterling Watson**, for being an amazing friend and research partner. I am always inspired by her can-do attitude, and it is because of her constant drive as a collaborator, supporter and teammate that our PV-EDR research project has come so far. I have learned so much from her, and I will never forget these two years we have spent working together. Here's to our countless PV-EDR work sessions in the MechE fishbowls.

- **Natasha Wright** for her everlasting selflessness. Though she constantly has things to do, she always made time for me, whether it was to help me understand the electrodialysis process better or message me on WhatsApp while I was in India trying to figure out an issue with the system. She not only catalyzed this research project before I began, but she is also one of the critical contributors to its success.

- **Sahil Shah**, for being a constant resource of knowledge, ideas and inspiration. He is a humble, yet model researcher and engineer. Everything I have seen him do is of the highest quality. Whenever I speak with him, I always wish I had his ability to analyze problems on the spot and suggest solutions.
- the rest of the PV-EDR team: **Professor Tonio Buonassisi**, **Marius Peters**, **Dev Ramanujan**, **Elizabeth Brownell**, and **Wei He** for all their ideas, guidance, and feedback that benefited this project and thesis.
- **Sree Rama** and **Nataraj** from Tata Projects for their tireless efforts to help install the PV-EDR system in Chelluru, collect data, debug the system, connect the piping network, and accompany me during my field work.
- **Nataraja**, **Harsha**, **Anil**, and **Tenny** from Tata Projects for their generous hospitality during my visits, feedback on my work, and thoughtful discussions on the future of desalination systems.
- the **GEAR Lab family** for being great friends and fellow researchers. Working with you all has been such an inspiring and humbling learning experience.

I would also like to thank the sponsors of this research and my graduate education:

- Tata Projects Limited
- United States Agency for International Development (USAID)
- Massachusetts Institute of Technology Energy Initiative (MITEI)
- Massachusetts Institute of Technology Tata Center for Technology and Design

Acknowledgment of Joint Work

This research project was done jointly and in collaboration with Sterling Watson. Our theses were prepared in parallel and share much of the same content, but I have crafted my thesis to reflect my individual focus and contributions.

Contents

List of Figures

List of Tables

Chapter 1

Introduction

This thesis investigates the design, development, and field-testing of a cost-optimized, village-scale, photovoltaic-powered electrodialysis reversal desalination system for rural India. It also details the models used to design the system and the interactions between the the power and desalination systems. The system was designed and constructed using off-the-shelf components and was installed and field-tested in Chelluru, a village approximately 70 kilometers northeast of Hyderabad, India.

The research contributions of this work include:

- A PV-EDR system model that predicts the cost and performance
- The cost-optimal PV-EDR system configuration that meets water demand given local input parameters such as salinity and solar irradiance
- Investigation into the sensitivity of the optimal PV-EDR system configuration and cost to system reliability and component costs
- System cost reductions enabled by flexible schedule operation and load sizing
- Installation of the PV-EDR system in the Chelluru and discussion of the results of a week-long field trial

1.1 India's Brackish Groundwater

In 2015, the WHO / UNICEF Joint Monitoring Programme (JMP) for Water Supply and Sanitation reported that 9% percent, or 663 million, of the global population does not use an improved drinking water source [1]. The JMP defines "improved" sources of drinking water as piped water into a dwelling, yard or plot of land, public taps or standpipes, tube wells or boreholes, protected dug wells or springs, or rainwater. Several examples of "unimproved" sources of drinking water are unprotected dug wells or springs, carts with small tanks or drums, tanker trucks, surface water, and bottled water [2]. However, a water source classified as "improved" is not necessarily safe to drink. The JMP 2015 Update reports that 7% of India's rural population does not even use or have access to improved water sources [1]. India has 600,000 inhabited villages that house 834 million people, or approximately 69% of India's population [3].

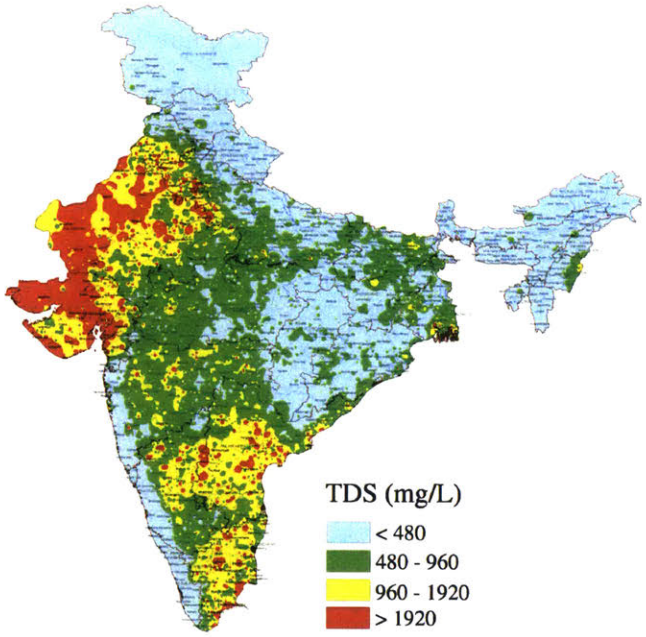

Figure 1-1: Map of groundwater salinity levels throughout India [4]

The Central Groundwater Board of India has compiled maps of the prevalence of each of the primary chemical contaminants in Indian groundwater throughout the country; namely salts, fluoride, nitrates, iron, and arsenic [4]. In doing so, it was found

that brackish groundwater, defined as water with a total dissolved solids (TDS) content between 500 and 30,000 mg/L, underlies approximately 60% of India's land area, as depicted in Figure 1-1. Village-scale desalination (in addition to other purification methods) could at least double the land area under which groundwater can acceptably be used as drinking water in India [5], which is not necessarily the equivalent of half the volume groundwater resources. The Bureau of Indian Standards for Drinking Water has set the acceptable upper limit for TDS to 500 mg/L for improved palatability and minimal risk of gastrointestinal irritation [6]. Some form of desalination is necessary to convert brackish groundwater into an acceptable drinking water source. For additional safety, microbial contamination can be eliminated through the use of disinfection methods such as UV exposure or chlorination.

1.2 Existing Desalination Solutions

1.2.1 On-Grid RO Systems

Tata Projects Limited, a sponsor of this research, has been working to mitigate the lack of access people have to safe drinking water sources. They have installed approximately 2,200 reverse osmosis (RO) systems, the large majority of which are grid-connected, in villages across India to desalinate the available water sources to safe drinking levels [7]. These village systems are typically funded and paid for by a local non-governmental organization (NGO). Off-grid systems cost more than double that of an equivalent capacity grid-connected system due to the addition of a photovoltaic power system. As a result, the NGOs opt to fund these water desalination systems for villages with semi-reliable grid electricity [7]. Therefore, if the cost of off-grid desalination systems could be reduced, it is reasonable to expect that more desalinations systems may be installed in villages without reliable grid connection, which are arguably in less fortunate circumstances.

As of 2015, 96.7% of Indian villages had been electrified, meaning they have some form of grid electricity [8]. However, the grid electricity in most villages is not reliable,

nor do many households benefit from it. In 2011, only 55.3% of rural households used electricity for lighting [9], which suggests that not all the households in electrified villages have reliable access to even basic electricity. And even those that do have access to electricity experience intermittent power outages and may only have access for a few hours per day.

Because of the limitations of the current electrical grid, on-grid rural water purification systems were designed to provide the daily water needs of the village in the limited number of hours of grid access typically available [5]. For example, if a village needs 10,000 liters of water per day and typically has 5 hours of grid electricity, then the RO system capacity would be designed to produce 2,000 liters per hour (LPH). On the other hand, if the village only has 1 hour of electricity, then the RO system would need a capacity of 10,000 LPH. Systems with greater water production capacity require higher power pumps and may require more RO membranes, resulting in a greater system capital cost. Therefore, the limitations of the electrical grid in some villages may render even grid-connected RO systems impractical or cost-prohibitive.

1.2.2 Off-Grid RO Systems

Because of the constraints of an unreliable grid, photovoltaic (PV) powered systems have become more attractive, especially in India, where there is a high average daily global horizontal irradiance solar resource of 6 kWh/m^2 [10]. However, photovoltaic-powered reverse osmosis (PV-RO) systems also have significant added costs due to the addition of the PV power system. The capital cost of a system varies depending on the specific village's needs, but as an example, an on-grid 500 LPH RO system costs about 300,000 INR (approximately $4,500 USD) while an off-grid 500 LPH PV-RO system costs about 750,000 INR (approximately $11,250 USD) [11]. When comparing similar capacity systems when designed for on-grid and off-grid villages, the cost of the off-grid PV-RO system is more than double that of the on-grid system. The inclusion of a PV power system contributes to more than half of the cost of a full PV-RO system, causing these PV-RO systems to also have prohibitively high capital costs for villages without sufficient access to the grid. One major contributor to the

power system cost of the PV-RO system is the high power and energy requirement of high pressure pumps that are required for RO.

1.3 Motivation for Photovoltaic-Powered Electrodialysis Desalination

Electrodialysis (ED), an alternative desalination process to reverse osmosis, uses an applied voltage across a stack of semi-permeable ion exchange membranes to transport ions, resulting in alternating streams of concentrate and diluate water. ED is expected to have a lower specific energy of desalination than RO for brackish water salinities below 5,000 mg/L. In fact, ED may require less than 50% of the energy used by RO to desalinate water below 2,000 mg/L [5], which constitutes the majority of India's brackish groundwater [4]. To first order, this implies that the cost of the power system of an off-grid electrodialysis system could be significantly reduced compared to an equivalent PV-RO system because of ED's lower energy requirement. These factors suggest that ED could provide a lower-cost, off-grid brackish water desalination solution [12].

In addition to energy savings, electrodialysis has other advantages compared to reverse osmosis. ED can reasonably achieve high recoveries of 80-90% compared to 30-60% typically achieved by RO. This leads to less water waste, an important factor given that India's groundwater resources are being depleted [13–15]. While RO membranes have an expected lifetime of 3-5 years, ED membranes have an expected lifetime of 10 years, meaning their recurring replacements costs may be lower on average despite being more expensive upfront. And finally, for off-grid, PV-powered systems, ED is more suitable than RO because PV generates power at a DC voltage, which could be applied directly to the stack without conversion to AC voltage.

Due to the constraints of unreliable grid electricity, the potential for photovoltaic-powered systems to mitigate this issue is appealing, particularly in India, where the solar resource is high [16, 17] (Figure 1-2), and solar is readily available and water

consumption is correlated with solar irradiance [5]. Solar energy is locally and indefinitely available, eliminating the need for consumable fuels such as diesel. PV panels also operate silently and without pollution to the environment and require minimal maintenance. Photovoltaics represent an autonomous and environmentally benign power source for off-grid power systems. Solar is the most abundant renewable energy source, and can serve as a low-maintenance energy source for regions without a reliable grid connection. While PV modules have historically been cost-prohibitive in many applications, particularly in emerging markets, PV module prices have declined by 10x during the 20 years and 100x during the last 40 years, enabling their use in these new markets [18].

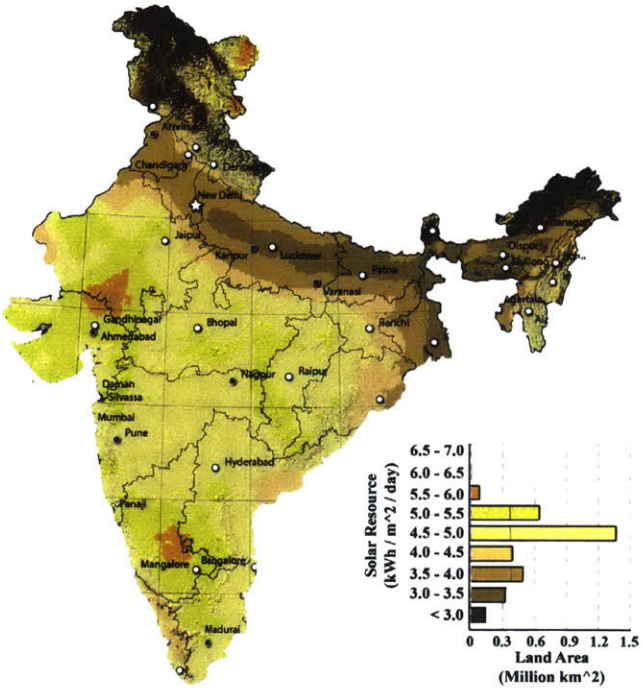

Figure 1-2: Map of solar irradiation in India [17]. The high solar resource makes photovoltaic-powered systems feasible in off-grid locations in India.

However, adapting existing systems to PV power in a cost-effective and reliable way is not always straightforward. While conventional energy sources and grid electricity are dispatchable and non-intermittent, PV is naturally intermittent and non-dispatchable. An electrical load designed to operate on a continuous conventional

energy source requires adaptation to operate with a variable PV power source. A storage medium can buffer the variability of the PV power source, rendering the availability of power to be predictable and persistent.

A key challenge in the field of PV-powered systems is to create systems that are simultaneously low-cost and sufficiently non-intermittent. Inadequate system design yields either higher cost (over-design) or lower reliability (under-design) [19]. PV-powered systems installed in remote locations such as rural Indian villages typically require both low cost and high reliability. On the other hand, co-design (as opposed to independent, disaggregated design) of the PV subsystem, storage media, and electrical load represents an opportunity for cost reductions and technological innovation. Furthermore, an opportunity exists to template key learnings in a system-design framework, to enable rapid development of a wide range of future optimized PV-powered systems. Cost reductions through system optimization are essential to accelerating PV-powered system adoption in low-income, remote environments, such as underdeveloped rural villages in India.

In these environments, the advantages of electrodialysis over reverse osmosis, namely lower energy requirement, higher water recovery and lower recurring costs of membranes, make electrodialysis a promising solution for off-grid desalination. In particular, combining the lower energy requirement of an electrodialysis system with a photovoltaic power system has the potential to reduce costs compared to an off-grid PV-RO system. Optimization of the combined PV and ED subsystems through detailed analysis of the interactions between the power production, energy storage, ED and pumping power requirements, and water storage presents an opportunity for further cost reductions and system design insights.

1.4 Prior Work

1.4.1 PV System Optimization

Previous work in the field of photovoltaic system optimization has focused on optimal power system sizing through simulation of electrical loads, power management, and PV power generation. Cost-optimized PV power systems for various applications have been studied and tested.

The techno-economic optimization of a PV power system for water pumping in Antalya, Turkey was studied by Olcan et al. [20]. This multi-objective optimization focused on minimizing the deficiency of power supply probability (DPSP) and the life-cycle costs. This study used a method of operating flexibly and using a water storage tank as a buffer. The optimal sizing of a different PV water pumping system with water storage for remote villages in Algeria was also investigated by Bakelli et al. [21]. A PV-wind-fuel cell RO unit was optimized in Smaoui et al. [22], but none of these studies have characterized the benefits of flexible operation and load sizing, which will be explored in this work in Chapter 3.

Habib et al. [23] optimized the sizing of the PV power system as well as the sizing and scheduling of electrical loads in a microgrid. The purpose of this work was to maximize solar energy utilization by scheduling loads accordingly. This approach, while in some respects similar to the work presented here, focused on the scheduling of multiple loads in the microgrid setting, rather than the optimization of a single PV-powered load. Load scheduling for a PV-powered microgrid was also investigated by Jaramillo et al. [24].

1.4.2 PV-Powered Desalination System Design

The use of PV power for ED and EDR systems has been studied in the past. Laboratory scale work has been completed to model and test a PV-ED system [25]. A number of field pilots have also been conducted. In 1987, Adiga et al. [26] completed a pilot PV-ED project with a production rate of 0.12 m^3/hr in the Thar Desert.

However, the water was only desalinated from 5,000 mg/L to 1,000 mg/L, well above the 500 mg/L drinking water requirement in India [6]. Because of the low charging and storage efficiency of batteries at the time and the high associated cost of a suitably sized PV system, batteries were omitted and the PV-ED system was designed to operate exclusively daylight hours (8:30AM - 4:30PM).

In the same year, Kuroda et al. [27] designed and constructed a batch mode PV-ED seawater desalination system in Nagasaki which operated around the clock from June 1986 to March 1988 to produce 2-5 m^3 of drinking water at 400 mg/L water per day. The aim was to optimize the system by matching its power consumption to the power generation of the PV panels. To do so, the system operated in two modes: a high-power mode to desalinate the seawater to moderate salinity during times of abundant solar irradiance, and a low-power mode to desalinate the moderate salinity water to 400 mg/L during times of low or nonexistent irradiance. Similarly, the battery capacity was optimized for utility by matching high power consumption for producing partially desalinated water during high power output times from the PV panels, and low power consumption for producing fresh water from the partially desalinated water during low power output times from the PV panels. Doing so justified using a smaller capacity battery compared to typically run electrodialysis systems. A few years later, Soma et al. [28] constructed a similar PV-ED system for brackish water desalination, and monitored the seasonal variation of water production.

Similar to the work presented in this thesis, both systems were designed with the motivation to minimize the cost of the PV-ED desalination system. However, the tests were conducted about thirty years ago, produced water of a higher salinity than our targets for an Indian village, and listed no concrete cost, power or energy consumption values for present-day comparison. Additionally, advancements in PV and battery technology have enabled different PV-ED configurations and at lower costs than what was previously achievable. These developments warrant a fresh, present-day investigation into cost-optimization and development of PV-ED desalination systems.

The aim of the research presented in this thesis was to develop an approach to op-

timally design a cost-effective PV-EDR system for rural India. In the literature, cost optimization of PV-powered reverse osmosis (RO) desalination systems is a related area of research. Bilton et al. [29–32] investigated the impacts of location-specific environmental and demand parameters on the optimal design of modular PV-RO desalination systems using genetic algorithms. They also worked extensively on examining energy generation methods considering not only PV, but also wind turbines and diesel generators, and optimizing them together with RO systems to determine a high-reliability system configuration with the lowest life cycle cost. The work presented in this thesis has similar goals in optimizing for minimal system cost while achieving high reliability of off-grid desalination systems in under-served communities. However, the performance and costs of components such as solar panels and batteries are generalized, rather than picking specific components from an inventory. Furthermore, the optimization analysis is focused on a single location, and the pilot system was designed, built and installed to evaluate its performance in the field.

1.5 Objectives and Thesis Outline

This thesis details the development, installation and testing of a photovoltaic-powered electrodialysis reversal (PV-EDR) desalination system in rural India. It presents the parametric theory and system modeling used to design a cost-optimized, constant voltage, and constant pumping power PV-EDR system that can be built from off-the-shelf components, as well as the development and field-testing process of the optimized system operating in the pilot location. We used GE Water's electrodialysis stack Model Number AQ3-1-2-50/35 [33], which was previously studied, modeled and tested by Wright et al. [12] and was readily available for this work. The system was chosen to operate in batch mode at constant voltage and constant pumping power power, as conventional electrodialysis systems are run. Off-the-shelf components were estimated by linear cost models and performance estimates based on data from OEMs and vendors. These data allowed us to establish a baseline for the lowest cost PV-EDR system that meets our desired requirements and can be built today. We can

further investigate a PV-EDR system with these characteristics to understand the cost sensitivities and determine where future research should be focused to enable further cost reductions. The theory, observations and results from this work will aid engineers in designing cost-effective PV-powered systems for other size scales and contexts.

This thesis also presents the benefits of flexible operation and optimal load sizing of a generalized off-grid, PV-powered process producing an accumulable output, as well as the application of these ideas to a field-tested PV-EDR desalination system. Here, the term "flexible operation" refers to the process's insensitivity to operating schedule, while "optimal load sizing" is the ability to design the load to operate at different power levels that complete the desired task over a corresponding duration.

This research culminated in the installation and field-testing of the PV-EDR system in the Indian village of Chelluru, a village about 70km northeast of Hyderabad. Chelluru has a population of approximately 2000 people, putting it in the median village population range of 2000-5000 people [34]. The groundwater salinity is 1600 mg/L, which is within the typical Indian groundwater range of 1000-2000 mg/L. Assuming 3 liters of daily water consumption per capita [35], the median village water requirement in India is 6-15 m^3. While Chelluru's average daily water demand is 6 m^3, this study aims to produce 10 m^3 in the interest of targeting the median village size. Finally, the product water salinity of 300 mg/L was selected for increased palatability, well below the Bureau of Indian Standards for Drinking Water recommendation of 500 mg/L [6].

To demonstrate the value of analyzing the coupled nature of the PV and EDR subsystems to cost-optimize the full system as a whole, we will compare the costs and design of (1) a PV-EDR system designed using a conventional design approach and (2) a PV-EDR system designed through optimization simulation using meteorological data. Both systems will be optimized for Chelluru to desalinate identical feed water and produce the same quantity and salinity of product water. By doing so, we will be able to fairly compare and assess the benefit of using optimization methods over conventional design methods for designing low-cost PV-EDR systems.

The following is an outline of this thesis:

- **Chapter 2: PV-EDR System Behavior**

  The basic theory behind the electrodialysis desalination process and photovoltaic power system operation to provide an understanding of the models used to predict the desalination process and the first-order energy analysis associated with designing power systems. Then the simulation model of their coupled behavior that evaluates a PV-EDR system's cost performance is summarized by breaking down the system analysis into modules consisting of electrodialysis, pump selection, power system, and cost.

- **Chapter 3: PV-EDR System Simulation Optimization**

  The simulation model described in Chapter 2 is coupled to an optimizer to find the lowest capital cost design for the given requirements and compared to a similar system that is designed through conventional means. The sensitivities of the optimized design to factors such as salinity, reliability and component costs are then explored through additional optimization studies. Then the cost benefits of a flexible operation schedule and load sizing is analyzed and discussed.

- **Chapter 4: Design and Field Testing**

  The field pilot system was installed and a week-long test was conducted. The results of this short-term test are presented and compared to what is expected in the model.

- **Chapter 5: Conclusions and Future Work**

  The results of this research as well as in-field observations are summarized, and suggestions for continuing and future work are outlined and presented.

Chapter 2

Photovoltaic-Powered Electrodialysis Reversal System Behavior

2.1 Electrodialysis System Behavior

Electrodialysis is the process of separating salts from water through the application of an electric potential across a series of alternating anion and cation exchange membranes (Figure 2-1). An ED system consists of the ED stack, pumps, and water storage and recirculation tanks. The ED stack is composed of cell pairs that are sandwiched between two electrodes, where a cell pair consists of an anion exchange membrane (AEM), a spacer for water flow, a cation exchange membrane (CEM) and another spacer. When running in batch mode, there are two recirculation tanks, one each for concentrate and diluate, respectively, and the water in these tanks is recirculated through the ED stack continuously until the desired diluate salinity is reached. Electrodialysis reversal (EDR) operates identically, with the addition of a reversal of the diluate and concentrate streams and a reversal of the stack voltage polarity. After a reversal, the diluate streams would be flowing in the channels where the concentrate streams flowed previously, and vice versa. In practice, this is done by changing valves to redirect water flow and reversing the polarity of the applied voltage. For this work, the ED stack used was manufactured by GE Water: Model Number AQ3-1-2-50/35, shown in Figure 2-2.

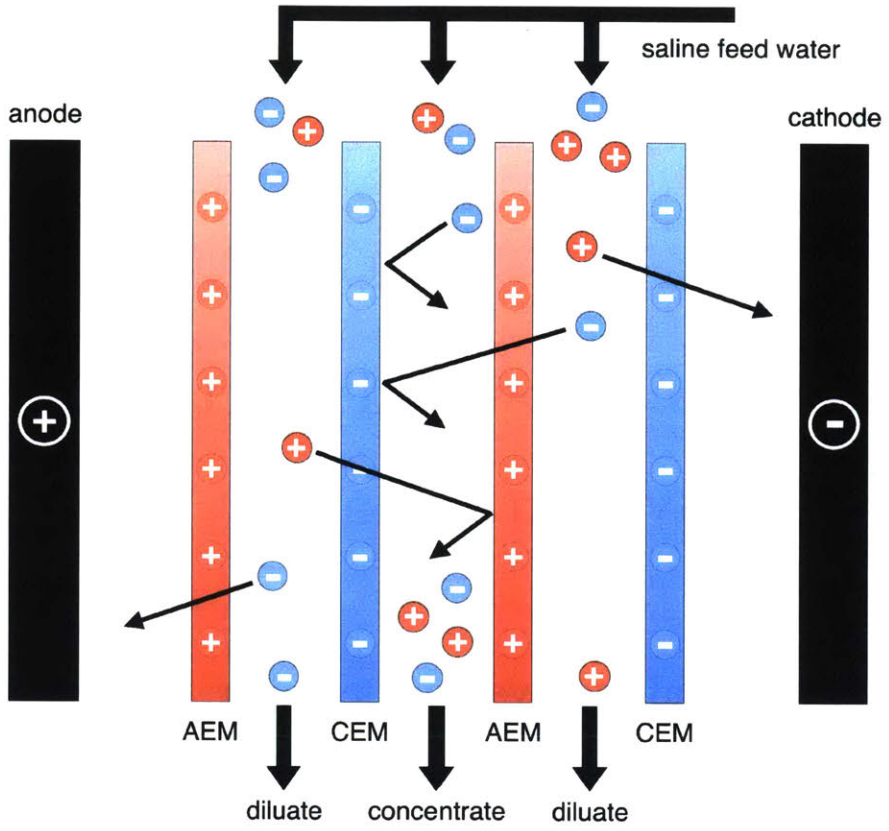

Figure 2-1: Electrodialysis separates salts from water through the application of an electric potential across a series of alternating anion and cation exchange membranes (AEM and CEM, respectively).

The models used for predicting the performance and behavior of batch electrodialysis systems in this work have been developed and validated by Wright and Shah [36]. In addition, it is suggested that the reader review Wright [37], Ortiz [38], Strathmann [39], and Tanaka [40] for a more complete understanding of the electrodialysis process. A few of the major concepts are summarized here to highlight their relevance to the overall optimization of the PV-EDR system. It is important to note that these models assume the dissolved salts in the water is purely sodium chloride (NaCl).

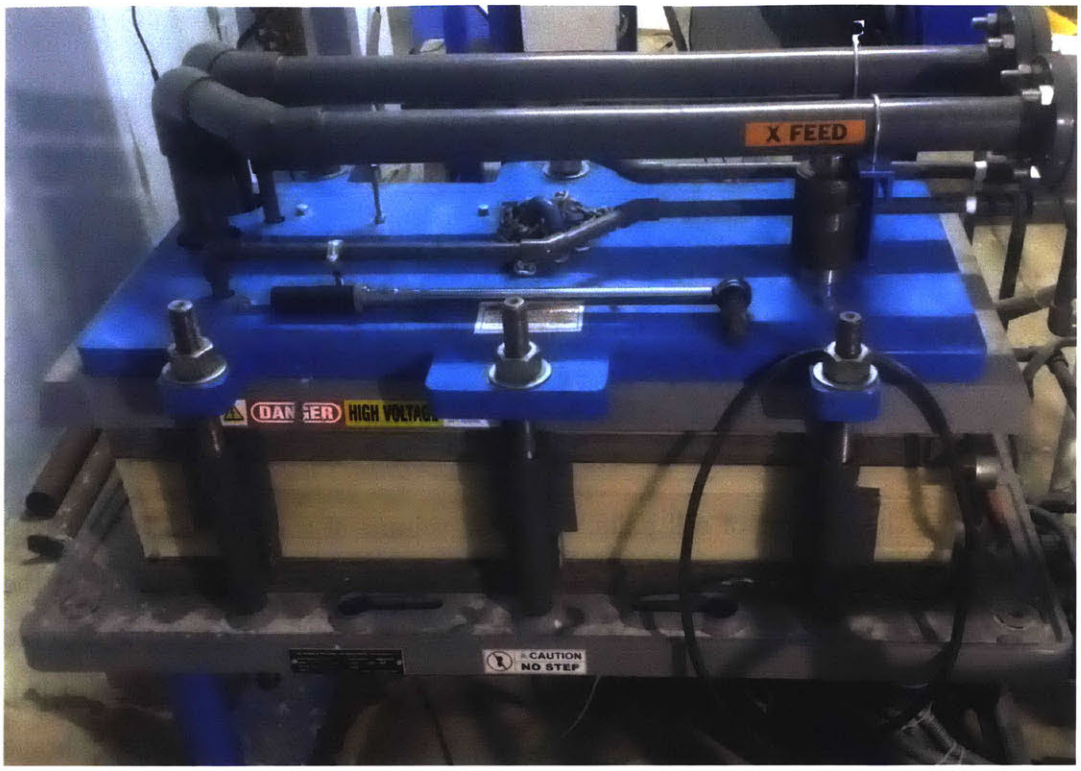

Figure 2-2: Electrodialysis stack. GE Water: Model Number AQ3-1-2-50/35 (modified).

2.1.1 Mass Transfer

The mass transfer of ions from one stream to another was modeled using Ohm's law. The electric potential is the voltage applied across the ED stack, the current is the ion movement, and the resistance is the electrical resistance of the membranes and the streams. Throughout an EDR batch, the current moves ions from the diluate stream into the concentrate stream, producing a change in concentration in time in both the diluate and concentrate channels (Figure 2-3a) according to the parameters in Table 2.1. Assuming equally-sized and equal numbers of concentrate and diluate channels and assuming perfect mixing within the recirculation tanks, the changes in concentration can be calculated using the mass balance analysis depicted in Equations 2.1 and 2.2 for the concentrate and diluate streams, respectively [38]:

$$N_k V_k \frac{dC_{conc}}{dt} = Q_{conc} C^0_{conc} - Q_{conc} C_{conc} + \frac{N_k \phi I}{zF} - \frac{N_k A D_a (C^{wa}_{conc} - C^{wa}_{dil})}{l_a} - \frac{N_k A D_c (C^{wc}_{conc} - C^{wc}_{dil})}{l_c} \quad (2.1)$$

$$N_k V_k \frac{dC_{dil}}{dt} = Q_{dil} C^0_{dil} - Q_{dil} C_{dil} + \frac{N_k \phi I}{zF} + \frac{N_k A D_a (C^{wa}_{conc} - C^{wa}_{dil})}{l_a} + \frac{N_k A D_c (C^{wc}_{conc} - C^{wc}_{dil})}{l_c}, \quad (2.2)$$

where N_k is the number of cell pairs, V_k is the volume of the streams (m^3), C^0_{conc}, C^0_{dil}, C_{conc}, C_{dil} are the concentrations of the concentrate and diluate streams at the inlet and outlet of the electrodialysis stack [mol/m^3], respectively, Q_{conc} and Q_{dil} are the volumetric flow rates [m^3/hour], ϕ is the current efficiency, I is the current [A], z is the charge of the ion, F is the Faraday constant, A is the active membrane area [m^2], D_a and D_c are the average diffusion coefficients [m^2/s] of NaCl in the anion and cation exchange membranes, respectively, l_a and l_c are the thicknesses [m] of the anion and cation exchange membranes, respectively, t is the time [s], and C^{wa}_{conc}, C^{wa}_{dil}, C^{wc}_{conc}, C^{wc}_{dil} are the concentrations [mol/m^3] on the surface of the anion and cation exchange membranes at the boundaries of the concentrate and diluate streams, respectively. These terms in the equation represent flow of ions at the inlet and outlet of the channels, the ion flow due to the current, and the diffusion of ions across the membranes due to the concentration gradient between the concentrate and diluate streams, respectively.

ED Variables and Parameters	**Quantity**
# ED Cell Pairs	62
Stack Voltage	45 V
Batch Size	0.42 m^3
Feed Water Salinity	1600 mg/L

Table 2.1: ED variables and parameters assumed for Figure 2-3.

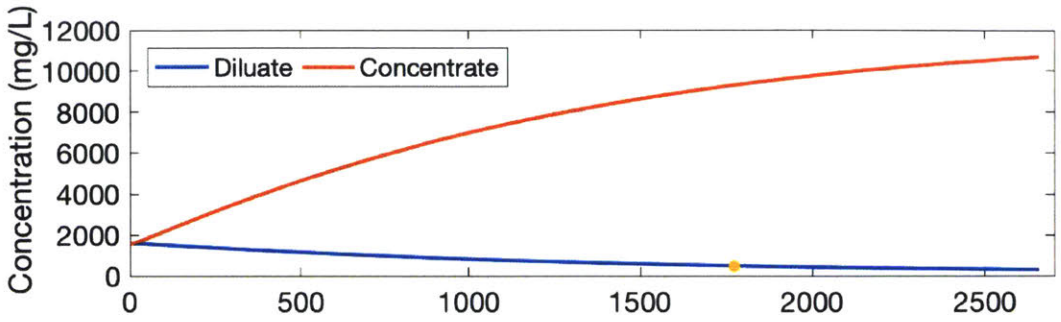

(a) Concentration of the diluate (blue) and concentrate (orange) streams during the ED batch process. The yellow dot on the diluate concentration curve indicates where the diluate crosses the 500 mg/L salinity threshold that is considered acceptable by the Bureau of Indian Standards for Drinking Water [6].

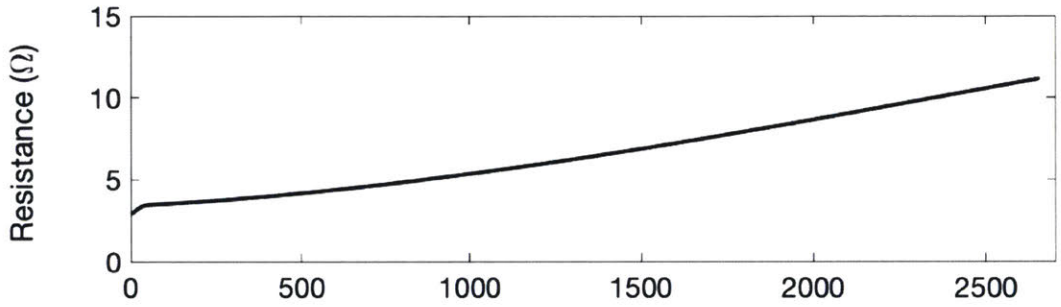

(b) Cumulative electrical resistance of the ED stack including during the ED batch process.

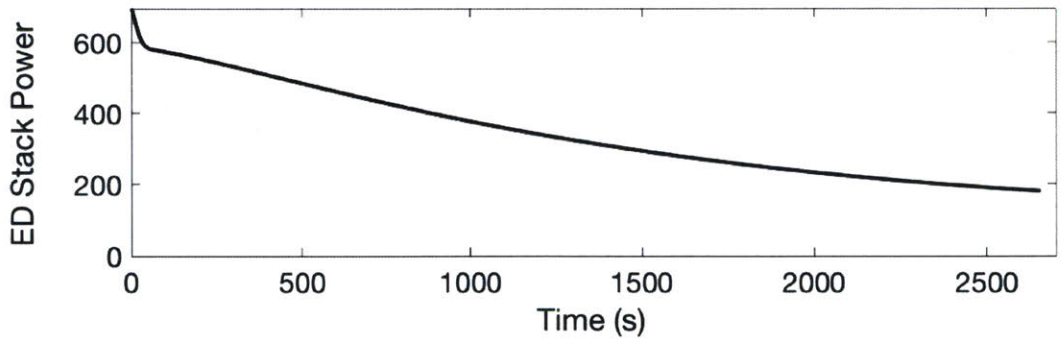

(c) ED stack power draw during the ED batch process.

Figure 2-3: As (a) the diluate concentration decreases, (b) the overall resistance of the stack increases, causing the current and thus (c) the stack power to decrease during the batch process. The variables and parameters assumed to create these figures are listed in Table 2.1. The figures depict the expected behavior of an ED system that is discussed later in Chapter 3.

As the concentrations of the concentrate and diluate streams change, their electrical resistances change. Due to the nonlinear relationship between resistivity and ion concentration, the diluate channels become the dominant resistance in the circuit, increasing electrical resistance overall (Figure 2-3b). During a batch process at constant voltage, this increasing resistance causes a decrease in current over time, slowing the desalination process of removing ions from the diluate stream. This causes the electrical power over the course of a batch to decrease proportionally with the current Figure 2-3c.

2.1.2 Limiting Current Density

If the applied voltage is too high, then at some point during the batch desalination process the ion concentration at the membrane surfaces in the diluate channels approaches zero. The condition during which this occurs is called limiting current density, which can result in electrolysis of the water molecules, causing harmful production of hydrogen gas and increased pH levels of the desalinated water. The ED system unit should be designed as to avoid reaching limiting current density at any point during the batch process. The limiting current density i_{lim} [A/m^2] is estimated using

$$i_{lim} = \frac{C_{dil}^{bulk} z F k}{T_{mem} - t}, \tag{2.3}$$

where C_{dil}^{bulk} is the concentration of the bulk diluate solution, t is the transport number of the ion in the bulk solution, and T_{mem} is the transport number of the ion in the membrane. k is the boundary-layer mass transfer coefficient [m/s] and increases with the linear flow velocity in the channels, causing a proportional increase in the limiting current density. In this analysis, the flow channels, membrane geometry and linear flow velocity are held constant. Holding these factors constant means that the limiting current density varies only with C_{dil}^{bulk}, which decreases over the course of the desalination process, and also that the pressure losses due to flow through the channels are also constant.

2.1.3 Electrodialysis System Design Considerations

For the purposes of this work, we are primarily concerned with desalinated water production rate and power profiles for the entire desalination batch process, which are the key factors that drive system cost and the value derived by the user. Desalination rate can be varied by changing (1) the applied voltage across the EDR stack and (2) the number of cell pairs.

At minimum, the applied voltage must be high enough to produce water with the desired salinity level such that the daily water production target is produced within 24 hours. However, the applied voltage must not be so high that limiting current density is reached during the desalination process.

The number of cell pairs effectively changes the number of channels and thus the volumetric flow rate, assuming a constant linear flow velocity through each channel. The range of optimal linear velocities for the spacers in our ED stack was 6-12 cm/s [33,41]. Because pressure drop per unit length of the spacer exhibits quadratic growth with increasing linear flow velocity, we chose to design our system to run at 6 cm/s primarily because it requires less pumping power per unit of flow rate. Additionally, lower linear flow rates are correlated with greater salt removal per unit length of spacer, which is beneficial for effective desalination [41].

The applied voltage and number of cell pairs therefore also determine the power and energy profiles associated with the desalination process. Varying these values only produces small differences in the total energy required per volume of drinking water. Assuming limiting current is not reached however, the power delivered to the stack is proportional to the applied voltage and stack current, and the pumping power varies proportionally with the number of cell pairs.

In this project, the maximum number of cell pairs in this study was limited to 170, which is the number of cell pairs available in the fully assembled GE Water ED stack. The recovery of the system was chosen to be 90% to minimize water wastage and is within the capabilities of electrodialysis.

2.2 Photovoltaic Power System Behavior

2.2.1 Photovoltaic-Powered Systems with Accumulable Output

A photovoltaic-powered system with accumulable output is any process for which an electrical load is powered by PV to produce an output that can be stored. The concrete example explored here is desalination, which produces storable potable water, while other applications include pumped water, drip irrigation, or any kind of material processing or manufacturing with the capability to be shut down or restarted as needed. Any process that uses energy to transform an input into a product and is indifferent to the time of day in which it is operated is applicable to this analysis.

Theoretical Reference System

As a reference system, assume a design consisting of a PV array, a battery bank, and a 1 kW electrical load producing an accumulable output from 8AM to 4PM daily (Figure 2-4). The PV array supplies power to the electrical load and the battery bank depending on the demands of each and the solar power available.

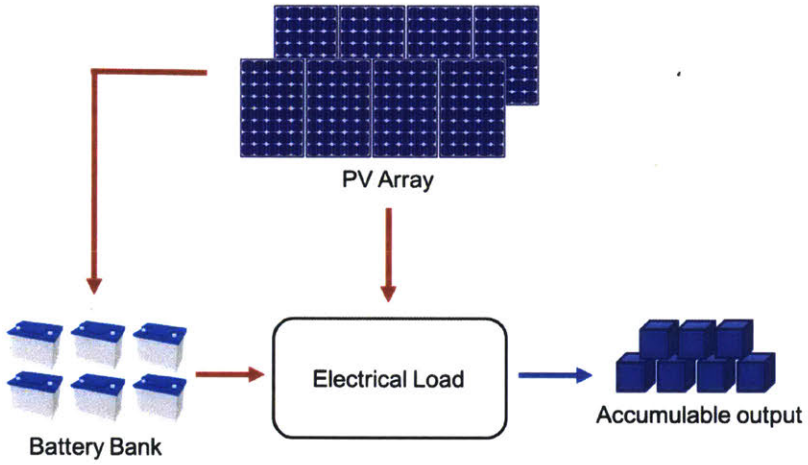

Figure 2-4: The theoretical reference system consisting of a PV array, a battery bank, and a 1 kW electrical load producing an accumulable output from 8AM to 4PM daily. The PV array powers the load directly and charges the battery if possible when solar irradiance is high, and the batteries power the load when the irradiance is insufficient.

Energetic Analysis

The power production of the PV array and the power consumption of the electrical load were used to determine the sizing of the battery bank through an energetic analysis. This section provides an explanation of how the PV power output is calculated, and how the energy storage requirement is calculated given an electrical load power profile.

Solar irradiance and temperature data for the region of Chelluru, India, in the year 2014 was used as a reference year's weather data throughout this thesis. This is semi-empirical satellite-based data from NSRDB [42]. The efficiency of the solar panels at each time interval, η_{PV}, was calculated using

$$\eta_{PV}(t) = \eta_{PV,nom}[1 + \alpha_p(T_{amb}(t) + k \cdot GHI(t) - T_{std})], \tag{2.4}$$

where $\eta_{PV,nom}$ is the nominal efficiency of the panels (15% is assumed in this analysis), α_p is the temperature coefficient [1/K] (-0.42% assumed in this analysis [43]), $T_{amb}(t)$ is the ambient temperature [°C], k is the Ross coefficient [K·m^2/W], which relates irradiance to module temperature ($k = 0.025$ for this analysis [44]), $GHI(t)$ is the global horizontal irradiance [W/m^2], and T_{std} is the standard testing temperature of 25°C. The power produced by one square meter of photovoltaic panels, $P_{PV,1m}$, was calculated by multiplying the instantaneous PV efficiency, η_{PV}, by the instantaneous global horizontal irradiance $GHI(t)$. The PV array power output, P_{PV}, is simply the product of $P_{PV,1m}$ and the area of the PV array.

The energy stored in the battery bank during charging was calculated using

$$E_{stored}(t) = E_{stored}(t-1) + \Delta t \cdot [P_{PV}(t) - \frac{P_{load}(t)}{\eta_{conv}}] \cdot \eta_{batt}, \tag{2.5}$$

and the energy stored during discharging was calculated according to [45]

$$E_{stored}(t) = E_{stored}(t-1) + \Delta t \cdot [\frac{P_{load}(t)}{\eta_{conv}} - P_{PV}(t)], \tag{2.6}$$

where E_{stored} is the energy stored in the batteries, Δt is the time interval in seconds

(300 seconds in this analysis), P_{load} is the power being consumed by the load [W], η_{conv} is the efficiency of the power converter, and η_{batt} is the battery charge/discharge efficiency. Temperature effects were not considered in the battery operation, which is acceptable in this analysis because the battery bank of the PV-EDR is stored out of direct sunlight.

2.2.2 Relationship Between PV and Batteries

As a first-order constraint, the output of the PV panels must be enough to produce the total amount of energy required to desalinate water over the yearly cycle. The minimum PV panel area required to do so, $A_{PV,min}$, can be found by taking the total energy required to desalinate a year's worth of water and dividing by the expected energy producible by one square meter of PV panels in a characteristic year, which is calculated to be 11 m^2 for the reference system. $A_{PV,min}$ corresponds to a design with the highest storage requirements, as all energy that is produced and not instantaneously used must be stored to ensure its use at a later time with none to spare at the end of the year.

By increasing the PV area beyond this theoretical minimum, the energy storage requirements can be reduced. The energy storage required for 100% output reliability of meeting the water or other product demand was found by simulating the energy stored over the course of the entire reference year according to Equations 2.5 and 2.6. As the PV area is increased beyond the minimum of 11 m^2, as plotted in Figure 2-5, the battery capacity required to buffer for intermittencies decreases [45]. All points along the curve in Figure 2-5(b) correspond to designs with equivalent output in the reference year.

There is a minimum-cost combination of PV panels and batteries that can supply the 8-hour, 1 kW fixed operating schedule reference system. This minimum-cost point lies on the curve represented in Figure 2-5(b) and Figure 2-6, and its value (indicated by the red ring in Figure 2-6) depends on the ratio of the cost of batteries and the cost of PV. The costs of PV panels and lead acid batteries throughout this analysis are \$98 per m^2 and \$150 per kWh, respectively, which are characteristic costs in

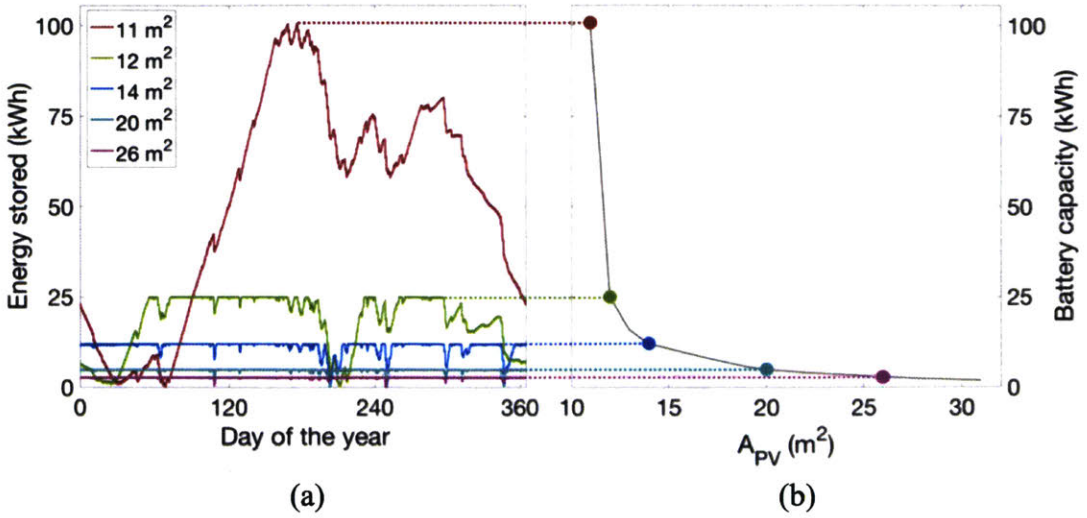

Figure 2-5: Relationship between PV area and minimum battery capacity. The energy stored for systems with various PV area over the course of the reference year; (b) the battery capacity requirement for each PV area. As PV area is increased beyond the minimum, the energy storage capacity requirement decreases.

India for multicrystalline silicon PV panels and lead acid batteries [46]. The curve in Figure 2-6 represents the locus of designs that will provide 100% output reliability for the reference year, where 100% output reliability means that water demand is perfectly met given the reference year's solar irradiance data. Alternatively, this represents a loss of power supply probability (LPSP) of 0, where LPSP is defined as the average fraction of time that the load is not supplied by the PV system [47]. In this analysis, the LPSP is calculated relative to a single reference year, 2014 weather data for Chelluru, India. In the figure, the parallel lines represent constant cost for the power system of PV panels and batteries, where their slope represents the ratio of energy storage cost per kilowatt-hour to PV cost per square meter, and cost increases as the quantity of batteries and PV increases (toward the upper-right corner of the plot). If the ratio of energy storage and PV cost shifts, then the ratio of energy storage and PV area in the lowest-cost design would shift along the constant output reliability curve. The region above the 100% output reliability curve corresponds to overdesigned power systems which can produce more than the required output over the course of the reference year, and the region below the curve corresponds to

unreliable systems that cannot produce the required output throughout the reference year.

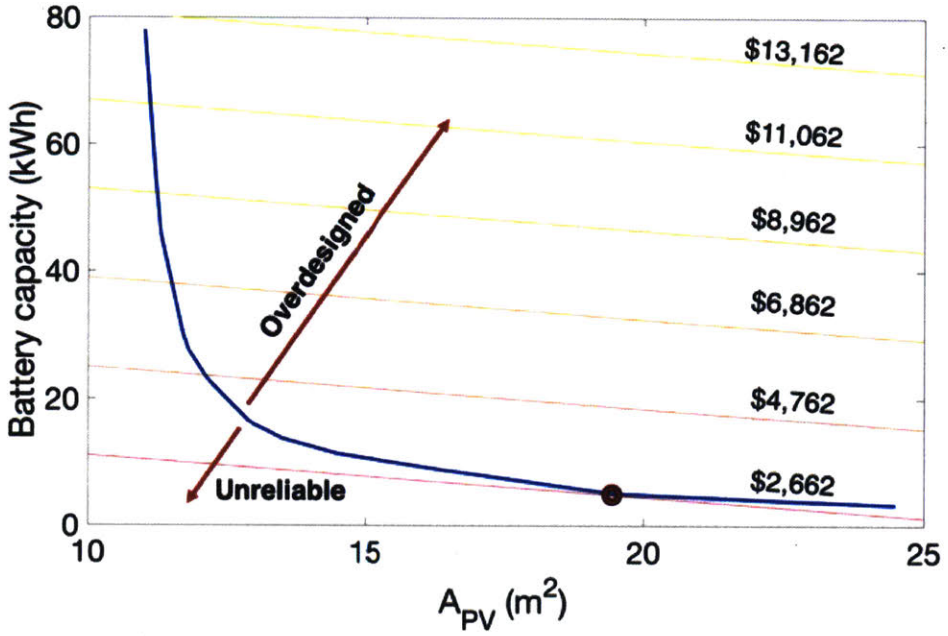

Figure 2-6: Power system configurations (PV panels and batteries) that can provide the required output with 100% reliability in the reference year. To the right of the curve are overdesigned systems which can provide excess output, and to the left of the curve are designs that cannot provide the required output over the course of the reference year. The diagonal lines represent constant cost power systems, and their slope is determined by the ratio of battery cost to PV panel cost. The lowest intersection point on the locus of power system designs in the direction orthogonal to the constant cost lines corresponds to the lowest-cost power system [45]. Here, the lowest cost power system configuration is $2,662.

2.2.3 Energy Storage and Product Storage

For processes that produce an accumulable output, storage of that output can serve as a secondary storage medium to energy storage in batteries. This can be done when the load is operated on a flexible schedule determined by the solar and battery energy available. Under certain conditions, utilizing product storage in addition to energy storage can allow for system cost reductions, as will be described in Chapter 3.

2.3 PV-EDR Coupled Behavior and Simulation Model

A PV-EDR model was developed using the theory from previous sections to inform the design of cost-minimized PV-EDR systems for any location, and to specifically optimize the off-grid, village-scale PV-EDR system for a median-sized village in India. This model is composed of four modules: the electrodialysis module, the pump selection module, the power system module, and the cost module. It was designed to take location-specific parameters and specified values of design variables as inputs, and produce a system capital cost and output reliability for the specific design. This process flow is depicted in Figure 2-7.

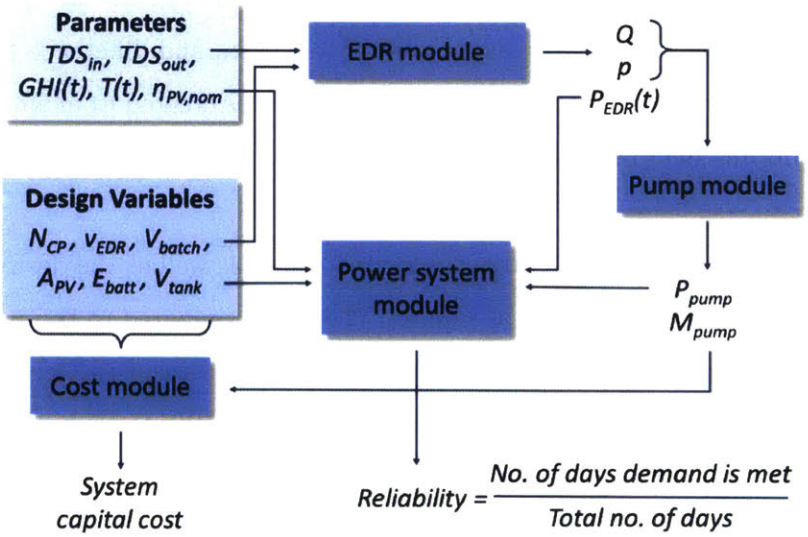

Figure 2-7: Flowchart of the PV-EDR Simulation Flowchart of the PV-EDR simulation, where TDS_{in} is the input salinity, TDS_{out} is the output salinity, GHI is the global horizontal irradiance, T is temperature, $\eta_{PV,nom}$ is the nominal PV efficiency, N_{CP} is the number of cell pairs, v_{EDR} is the stack voltage, V_{batch} is the batch volume, A_{PV} is the area of the PV array, E_{batt} is the battery capacity, V_{tank} is the water storage tank volume, Q is the flow rate, p is the pressure, P_{EDR} is the power required for EDR over a batch, P_{pump} is the pumping power, and M_{pump} is the pump model.

2.3.1 Electrodialysis Module

The EDR module simulates the water desalination process. To do so, it takes the feed water salinity TDS_{in}, desired output water salinity TDS_{out}, and desired average daily

water production as fixed inputs, and the number of cell pairs N_{CP}, applied stack voltage v_{EDR}, and batch size V_{batch} as design variables. The module then calculates and outputs the duration of a batch, water production rate, power profile P_{EDR}, the percentage of time that limiting current density was exceeded, and the flow rate and pressure required of the pumps. A design fails in the EDR module if the limiting current density is exceeded or if the desired salinity of the batch is not reached in sufficient time to allow the daily water production to be achievable.

2.3.2 Pump Selection Module

Based on the flow and pressure requirements of the ED system, an optimal pump must be chosen that minimizes cost, power consumption, and difference between the actual and the desired flow and pressure. A database was created from which to select specific pump models due to a poor correlation between pump performance metrics and cost.

The pump selection module takes the system curve as well as the desired pressure and flow rate of the EDR system as inputs. These are compared to the pump curves of the pumps in the database. The intersection points represent the expected actual operating point of the pump. A pump selection metric (PSM) (Equation 2.7), was created to evaluate the quality of choice of the pump based on pump cost, power consumption and the difference between the flow rate at the intersection to the desired flow rate.

$$PSM = C_{pump} + 3P_{pump} + 750|Q_{desired} - Q_{actual}| \tag{2.7}$$

Minimizing the cost of the pump directly translates to capital cost reductions. Minimizing the nominal power of the pump translates to capital cost reductions due to lower power system requirements. Minimizing the difference between the actual and desired flow rate will decrease the likelihood of the desalination process becoming affected due to a greatly different flow rate. The cost coefficient is 1 because it has a direct correlation to the overall system capital cost. The power coefficient is 3

because it is estimated that a small microgrid costs \$3/W of power generating capacity, [48, 49], and it is estimated here that the power consumption of the pump would add approximately \$3/W of cost to the PV power system. The flow rate difference coefficient of 750 was determined through numerical comparison demonstrating that it was sufficiently high such that the flow differential would be unlikely to exceed 0.1 m^3/hour and thus would be unlikely to significantly change neither the predicted pumping pressure required nor the desalination process. The pump in the database with the lowest PSM value for the desired flow rate and pressure is chosen for the design.

2.3.3 Power System Module

Solar is an intermittent power source that varies on daily and seasonal scales. A PV-powered system must have the energy storage capacity to provide the required power to the load despite fluctuations on the daily scale (such as clouds and nighttime operation) and variations on the yearly scale, such as lower solar irradiance during the winter season. A combination of PV panels and batteries can meet the power supply profile of a prolonged electrical load. The optimal sizing of the PV array and battery pack depends on location-specific weather data such as irradiance and ambient temperature, the power profile of the load, and the relative cost of PV and batteries.

The power system module uses time-resolved solar irradiance $GHI(t)$, time resolved temperature data $T(t)$, and nominal PV efficiency $\eta_{PV,nom}$ as parameter inputs to Equation 2.4 to calculate the estimated PV efficiency $\eta_{PV}(t)$. Design-specific values of PV array area A_{PV}, battery capacity E_{batt}, and water storage tank volume V_{tank}, as well as the power profiles of the EDR unit $P_{EDR}(t)$ and pump $P_{pump}(t)$ are fed into the module. The energy flow into and out of the batteries and the water flow into and out of the water storage tanks are simulated over the reference year period, and an output reliability corresponding to the percentage of days over the year for which water supply meets demand was calculated. The simulation will decide when to run a batch, simulate the charging and discharging of the batteries, and simulate

the water withdrawal over the course of a day according to the logic tree depicted in Figure 2-8. Within the simulation, the battery maximum discharge depth allowed is 50%, a value selected to prolong battery lifetime.

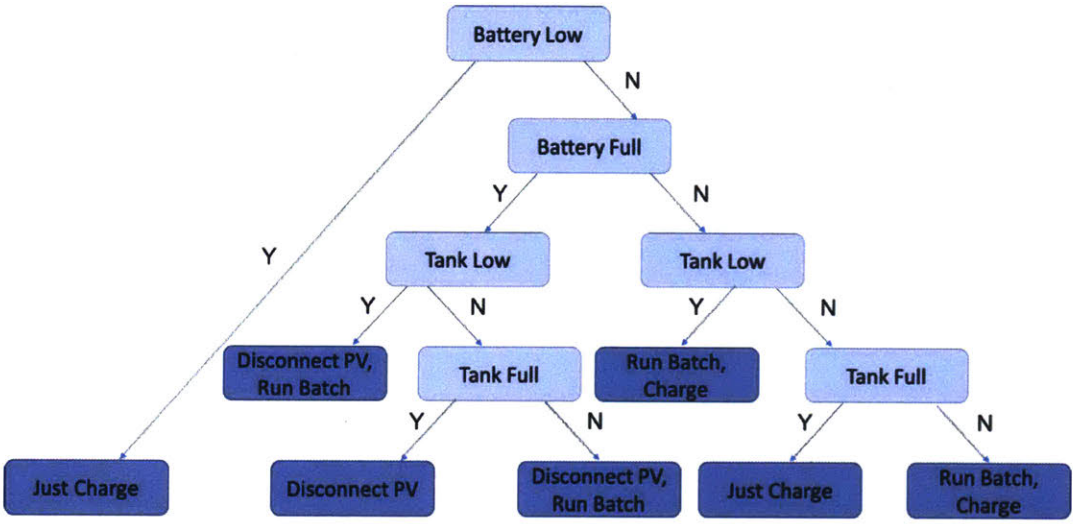

Figure 2-8: Power System Logic Tree Logic tree for the power system module, detailing the conditions for charging the batteries and running an EDR batch.

2.3.4 Cost Module

The cost module calculates the cost of the PV-EDR system based on the design variables and the selected pump according to Equation 2.8 using the costs in Table 2.2.

$$C_{sys} = C_{PV}A_{PV} + C_{batt}E_{batt} + C_{tank}V_{tank} + C_{CP}N_{CP} + 2C_{elec} + 2C_{pump} \qquad (2.8)$$

In Equation 2.8, C_{sys} is the system capital cost; C_{PV}, C_{batt}, C_{tank}, C_{CP}, C_{elec}, and C_{pump}, are the cost of the PV array, battery bank, water storage tank, membrane cell pairs, electrodes, and pumps respectively; and A_{PV} is the area of the PV array [m^2], E_{batt} is the battery capacity [kWh], V_{tank} is the water storage tank volume [m^3], and N_{CP} is the number of membrane cell pairs. An inverter suitable for the optimized power system and EDR and pumping loads was selected retroactively and

its cost was not included in the analysis presented in this thesis, though it would add to the actual total system cost. The cost of PV, batteries, and water storage were all determined based on local or commonly used component costs. The cost of ED cell pairs and electrodes ($2000 per electrode) are based on estimates from supplier quotations for the GE Model Number AQ3-1-2-50/35 ED stack [50]. The membranes are approximately 0.47 m^2, so a cost of $150/cell pair translates approximately to $160/$m^2$ (two membranes per cell pair).

Design Variable	Symbol	Cost
PV Area	A_{PV}	$98/$m^2$ [46]
Battery Capacity	E_{batt}	$150/kWh [46]
Water Storage Volume	V_{tank}	$110/$m^3$ [11]
# ED Cell Pairs	N_{CP}	$150/cell pair [50]
Stack Voltage	v_{EDR}	N/A
Batch Size	V_{batch}	N/A
Pump Model	M_{pump}	N/A

Table 2.2: Design variables that define a PV-EDR system and their associated costs per unit.

2.3.5 System Simulation Model

The performance of a PV-EDR design over a reference year was simulated in Matlab. The input parameters for the simulation given in Table 2.3 are primarily targeted at the median-sized Indian village, though the input salinity and solar irradiance are specific to Chelluru. The solar irradiance and temperature data used for all simulations was obtained from the National Solar Radiation Database (NSRDB) SUNY database for the village of Chelluru, India in 2014 [42], and interpolated to 5-minute intervals . All references to water production reliability are defined as the percentage of days that the simulation predicted the system would be able to provide the needed quantity of water under the weather conditions of the 2014 reference year. The water collection model assumes 0.25 m^3 of water is collected instantaneously every 15 minutes over the course of 10 hours during the day, resulting in 10 m^3 per day, with

the simplifying assumption that there is no seasonal variability.

Parameter	Symbol	Value
Input Salinity	TDS_{in}	1600 mg/L
Output Salinity	TDS_{out}	300 mg/L
Daily Water Production	V_{prod}	10 m^3
Water Production Reliability	r_{req}	100%
Solar Irradiance	$GHI(t)$	2014 GHI data for Chelluru
Ambient Temperature	$T(t)$	2014 data for Chelluru
Nominal PV Efficiency	$\eta_{PV,nom}$	15%

Table 2.3: Input parameters for the PV-EDR simulation, specific to conditions at the Chelluru test site.

Just as the power production and availability of the PV system can be tuned by the sizing of the panels and batteries, the power consumption of the ED system can be tuned by selecting the quantity of membrane cell pairs, operating voltage, batch size, tank size, and pump model. By jointly adjusting power production and power consumption, the power profiles can be matched in such a way as to optimize the overall system for minimum cost. Harvested energy can be (1) stored in batteries for later use or (2) used immediately for desalination, storing the excess water in tanks to meet customer demand at times of low irradiance. Incorporating water storage tanks as a secondary storage medium to batteries can reduce the battery energy storage requirement for the system as well as the overall cost of the system. This simulation model will be utilized in the following chapter for cost optimization studies.

Chapter 3

PV-EDR System Optimization

A PV-EDR simulation model was developed in Chapter 2 to take design parameters such as location-specific parameters and specified values of design variables as inputs, and produce a system capital cost and output reliability for the specific design. When coupled to a particle swarm optimization algorithm, multiple designs are randomly initialized and then varied and eventually converge on a low-cost design with acceptable reliability. A PV-EDR design was characterized as a combination of the design variables listed in Table 2.2. Due to the coupled nature of the PV and EDR subsystems, it is nontrivial to determine what configuration of the ED stack, pump models, and quantities of PV panels, batteries, and water storage tanks will result in the lowest capital cost system, and a full-factorial study would be too time-consuming and inefficient. Coupling an optimizer algorithm with the PV-EDR performance models can more efficiently determine the cost-optimal, or near-cost-optimal, combination of these components and the accompanying operational specifications.

3.1 System Cost Optimization

3.1.1 Particle Swarm Optimization

Particle swarm optimization (PSO) is a heuristic optimization approach that iteratively adjusts a population of randomly selected designs (comprised of a defined

set of design variables) based on their performance to an objective function [51]. It was selected for this application because of its suitability to searching a complex design space using stochastic methods, and the simplicity of implementation. It was straightforward to couple the PSO algorithm to the PV-EDR simulation.

For the purposes of optimization, days that failed to supply the water demand were penalized by adding $1,000 to the system cost for each of the N_{failed} failed days. Thus, the $1,000 per failed day penalty encourages the optimizer to find designs with minimal failed days. This changes Equation 2.8 to Equation 3.1

$$C_{sys} = C_{PV}A_{PV} + C_{batt}E_{batt} + C_{tank}V_{tank} + C_{CP}N_{CP} + 2C_{elec} + 2C_{pump} + 1000N_{failed} \tag{3.1}$$

3.1.2 The Optimized PV-EDR System

PSO was used to determine a cost-optimal PV-EDR design for any given set of parameters and design variables. Due to the stochastic nature of PSO, the optimization converged to a different solution every time it was run. To identify the likely global minimum solution, the optimization was run several times to identify the most promising regions of the design space. The design variable bounds were constricted so the optimization would constrained to exclusively search in those narrowed regions of the design space to find the cost-minimum design. Table 3.1 shows the results of the PV-EDR optimization for a system satisfying the design parameters listed in Table 2.3, and the cost breakdown of components is shown in Figure 3-2.

The simulated performance of the optimized PV-EDR design over the reference year is shown in Figure 3-1. To sustain a long operating lifetime of the batteries, the maximum depth of discharge allowed was set to 50%. During times of low irradiance when the battery was depleted to that level, the water stored in the tank would begin to be withdrawn, serving as a buffer until the batteries could regain charge. This mode of operation will allow the system to provide the daily water requirement of 10 m^3.

Design Variable	Symbol	Quantity
PV Area	A_{PV}	57.5 m^2
Battery Capacity	E_{batt}	22 kWh
Water Storage Volume	V_{tank}	10 m^3
# ED Cell Pairs	N_{CP}	62 cell pairs
Stack Voltage	v_{EDR}	45 V
Batch Size	V_{batch}	0.42 m^3
Pump Model	M_{pump}	Kirloskar Wonder III (x2)
Total Cost	**$23,420**	

Table 3.1: Design variable values for the lowest-cost PV-EDR system found through PSO iteration. The total system cost based on these optimized system design variables was $23,420.

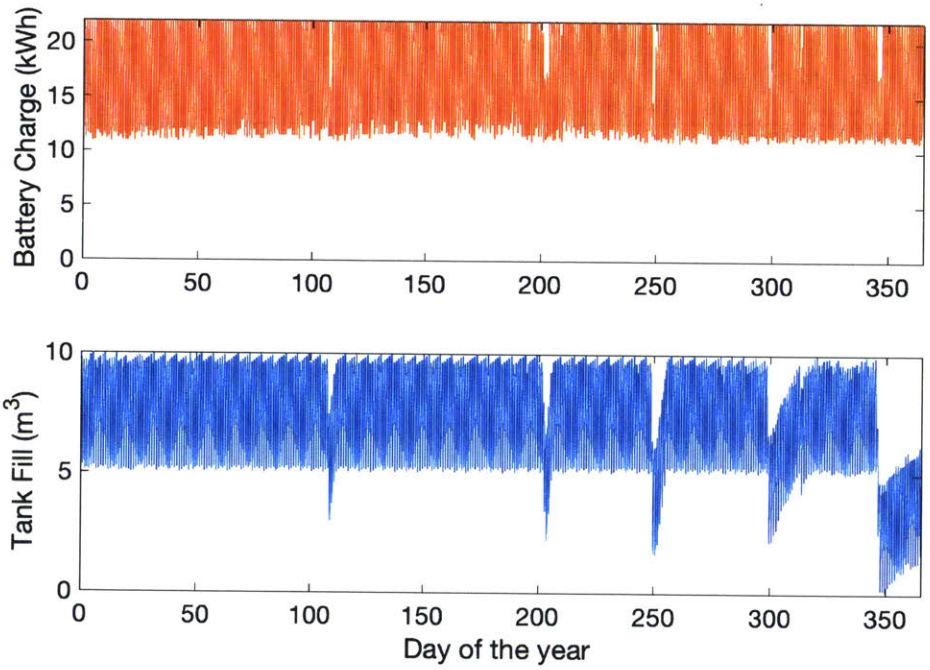

Figure 3-1: Simulated battery charge level and tank fill level for the optimized PV-EDR design during the reference year.

3.1.3 Levelized Water Cost

The levelized cost of water is typically calculated using the full system capital costs, facility costs, operation and maintenance costs, component replacement and other

variable costs, and interest rates [52]. Here, only the initial major system components and their replacement costs are considered, as many of the other factors such as transportation, construction, installation, and operation costs are still unknown. The partial levelized water cost estimation presented here assumes a system lifetime of 20 years, time-independent component costs, and unfailing operation over the full system lifetime. The components considered, their associated costs, assumed lifetimes, and the estimated numbers of times the components are purchased (including the initial purchase) over the course of 20 years are given in Table 3.2. This is assuming the design of the optimized system defined in the previous subsection.

Components	Quantity	Cost	Lifetime (years)	# of Times Purchased
PV Panels	57.5 m^2	\$98/m^2	20+	1
Batteries	22 kWh	\$150/kWh	5	4
Water Storage	10 m^3	\$110/m^3	20+	1
ED Electrodes	2	\$2000/electrode	10	2
# ED Cell Pairs	62 cell pairs	\$150/cell pair	10	2
Pump	2	\$44/each	3.5	6
Total Lifetime Cost			**\$47,063**	

Table 3.2: The components considered, their associated costs, assumed lifetimes, and the estimated numbers of times the components are purchased (including the initial purchase) over the course of 20 years. The lifetime cost is \$47,063 for a lifetime water production of 73,000 m^3 of water, resulting in a partial levelized water cost of \$0.645/m^3.

During its 20-year lifetime, the system is assumed to produce 73,000 m^3 of water (10 m^3 a day for 365 days a year for 20 years). With a lifetime cost of \$47,063, this results in a partial levelized water cost of \$0.645/m^3. Though many factors that are not included would add to this cost, it is still a reasonable value compared to the \$0.58/m^3 water cost claimed of another brackish water ED system [53, 54], given that the conditions under which that cost was calculated is also unknown.

3.2 Comparison of Optimized Design to PV-EDR System Designed Using Conventional Methods

For comparison, let the optimized design found in the previous section be referred to as Design A, in which the optimization and design of the PV and EDR subsystems were performed jointly, resulting in the design of a co-optimized system. Because village-scale PV-EDR systems are not currently commercialized in the field, the cost of a PV-EDR system with all the same input and desired output parameters when designed using conventional methods was calculated. This design will be referred to as Design B, in which the EDR system is designed first, and the PV power system is designed subsequently based on the power requirements of the EDR system.

Design A has been detailed in the previous section. For Design B, the EDR system was sized based on two criteria: the daily water production requirement of the median Indian village of 10,000 liters (10 m^3), and an average operation period of 8 hours per day (consistent with the operation period of the on-grid RO system at the test site). Correspondingly, the nominal flow rate of product water was chosen to be 1,250 liters per hour (LPH). The electrodialysis model was used to find the lowest-cost ED stack (when considered independently from the PV system) capable of producing 10 m^3 per day at a 1,250 LPH production rate. This high production rate requires an approximately proportional increase of 2.5 times in the number of electrodialysis cell pairs and applied stack voltage compared to Design A (140 cell pairs and a stack voltage of 100 V). However, the number of cell pairs was slightly reduced by increasing the applied voltage per cell pair, resulting in 136 cell pairs and a stack voltage of 98 V. This modification was motivated by the decreased cost of the EDR system by decreasing the number of cell pairs. The batch size was chosen to be 1 m^3 because it is a commonly used tank size and it could be desalinated and sent to the water storage tank in less than an hour. A suitable pump was suggested by Tata Projects, our industry partner, based on pumps they commonly use for their water purification systems and their knowledge of the local market. In summary, an EDR stack with a production rate of 1,250 LPH, a 1 m^3 batch size, and 136 cell pairs was

selected using this simplified, disaggregated approach. This EDR design had a daily energy requirement, $E_{EDR,d}$, of 20 kWh per day.

To design the power system, a battery capable of providing two days of backup was used [55]. This resulted in an energy usage requirement of $2 \cdot 20$ kWh $= 40$ kWh, resulting in a total battery capacity of 80 kWh assuming a 50% discharge depth. India's average daily global horizontal irradiance solar resource for the region under consideration, $E_{PV,d}$, is 6 kWh/m^2 per day [10]. This average was used to calculate the required area of PV panels according to

$$A_{PV} = 1.3\frac{E_{EDR,d}}{\eta_{PV} E_{PV,d}}, \tag{3.2}$$

where 1.3 is a scaling factor to account for losses [55]. In this case, $A_{PV} = 28.9$ m^2. For water storage, an industry standard 5 m^3 tank is assumed. The design variables of Design B are shown in Table 3.3 and the total system cost was calculated using Equation 2.8 to be \$40,138. The breakdown of cost by system components is shown in Figure 3-2.

Design Variable	**Symbol**	**Quantity**
PV Area	A_{PV}	28.9 m^2
Battery Capacity	E_{batt}	80 kWh
Water Storage Volume	V_{tank}	5 m^3
# ED Cell Pairs	N_{CP}	136 cell pairs
Stack Voltage	v_{EDR}	98 V
Batch Size	V_{batch}	1 m^3
Pump Model	M_{pump}	CNP CHL 2-30 (x2)
Total Cost	**\$40,138**	

Table 3.3: Design variables for Design B, the PV-EDR system found through conventional design methods. The total system cost based on these design variables was \$40,138.

A simulation of the performance of Design B over the reference year is shown in Figure 3-3. It is evident that the battery capacity is highly over-sized, such that the water storage is at no point utilized for buffering.

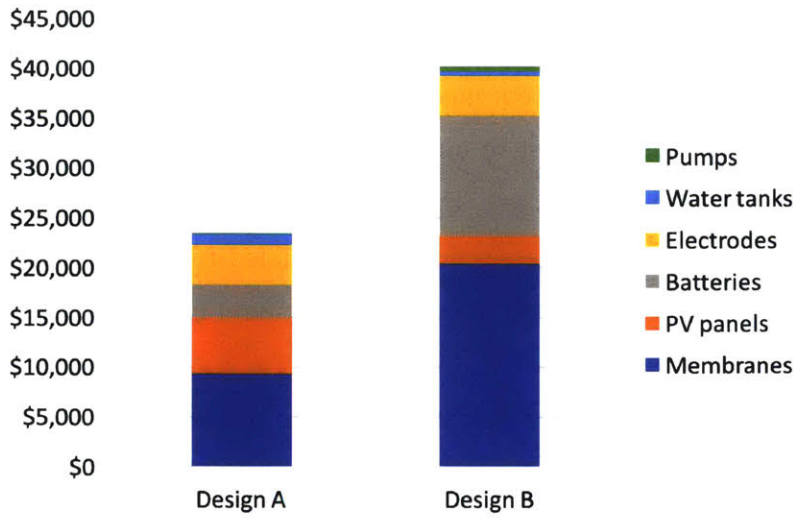

Figure 3-2: Comparison of cost breakdowns for Design A, the optimized system ($23,420 total), and Design B, the conventionally designed system ($40,138). Design B has a much larger ED stack which contributes significantly to its capital cost, as well as a much larger battery bank.

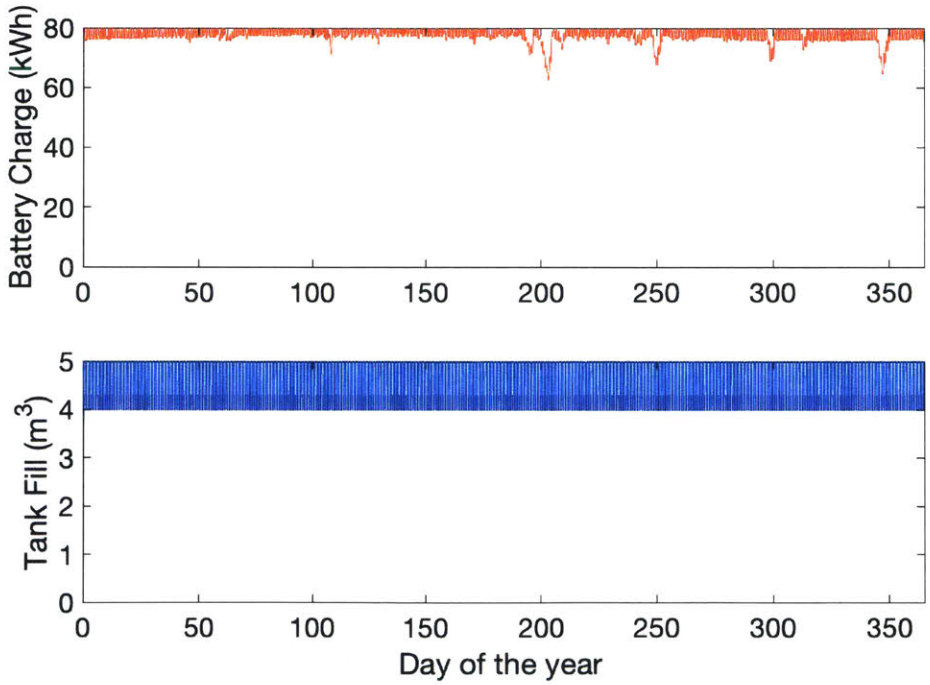

Figure 3-3: Simulation of the battery charge level and tank fill level for Design B during the reference year.

3.3 Cost Sensitivity Analysis

We used our PV and EDR system models and optimization tools to investigate the sensitivity of system capital cost to input parameters such as water output reliability and individual component cost. Each data point was produced by running the PSO optimization multiple times to find the associated total system cost. It is also important to note that each data point differs not only in cost, but also in system configuration.

As the output reliability constraint of 100% is relaxed, the capital cost drops quickly at first as shown in Figure 3-4, suggesting that just a few days of low sunshine are responsible for an disproportionate fraction of the system cost.

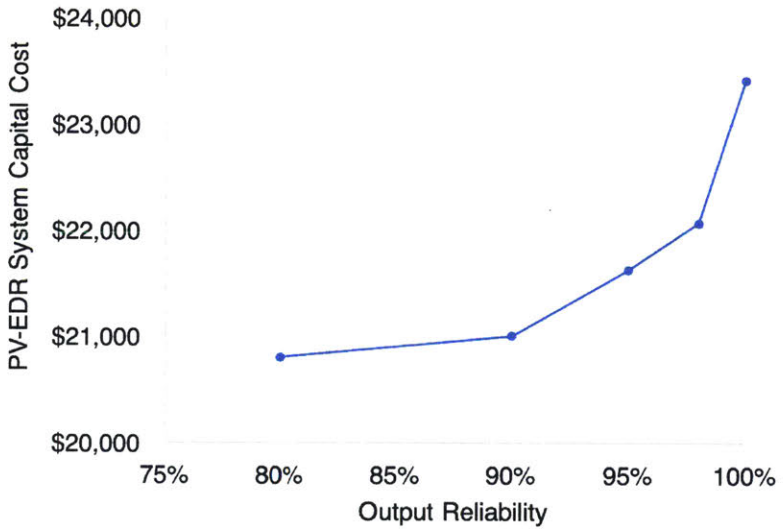

Figure 3-4: Sensitivity of PV-EDR capital cost to daily water output reliability. Reducing output reliability from 100% to 98% (7 days of the year in which the system fails to provide 10 m^3) produces a optimized cost reduction of 5.7% from $23,420 to $22,076, a relatively sharp drop compared to the 10.3% cost reduction for 90% reliability (36 failed days) to an optimized cost of $21,013.

The optimization was also run for various reductions in component capital cost for the batteries, PV panels, and ED membranes. The impact of these component cost reductions on total system capital cost is shown in Figure 3-5. It is evident that the total system capital cost is most sensitive to the cost of the membranes, relative

to the cost of batteries or PV panels. In particular, the nonlinear reduction in system capital cost with linear reduction in ED membrane cost indicates that the system design configuration changed, and the implications of this will be discussed in the next section.

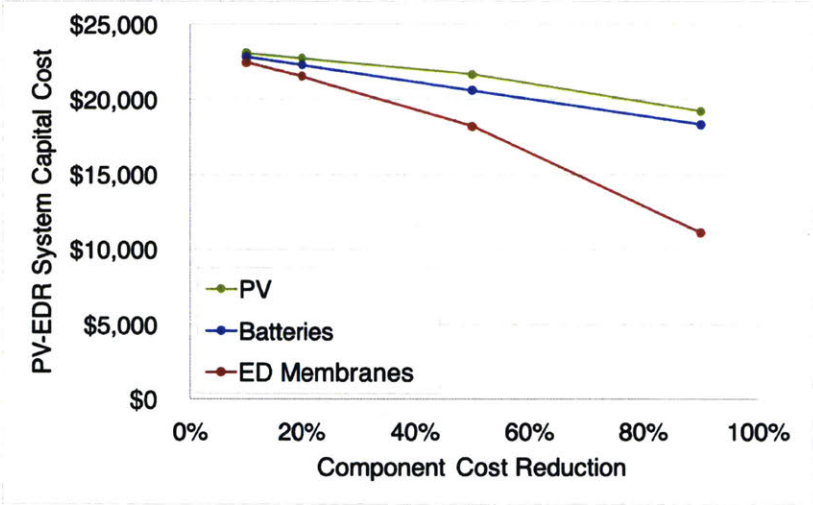

Figure 3-5: Sensitivity of PV-EDR capital cost to individual component cost reductions of batteries, PV, and EDR membranes by 10%, 20%, 50% and 90%. For each data point, the cost of all other components is held constant at the previously defined cost values.

3.4 Advantages of Operation Flexibility and Load Sizing for PV-EDR Systems

3.4.1 Cost Optimal PV-EDR System with Reduced Membrane Costs

As discussed in earlier sections, the optimized PV-EDR system had an average operating time of 17.7 hours per day. Desalination rate is proportional to the number of EDR membrane cell pairs that make up the EDR unit. To produce the necessary 10,000 liters of product water per day, the optimized PV-EDR system was required to operate for this duration. Figure 3-8 illustrates the frequency of number of hours

operated per day for the optimized PV-EDR system. Aside from several outliers, the system was expected to run 17.7 hours every day. The optimization converged on this design with a long operation schedule because it allowed for a smaller EDR unit, which was favorable due to the current high capital cost of ED membranes.

However, it is not unreasonable to assume that ED membrane costs will drop significantly compared to the current cost of the membranes used in the GE electrodialysis stack. In fact, according to supplier quotations from Hangzhou Iontech Environmental Technology, current prices for similarly sized ion-exchange membranes used in ED stacks are estimated to $40 per cell pair [56]. Since the membranes are approximately 0.64 m^2, this translates to a cost of $31.25/$m^2$ (two membranes per cell pair), more than 80% less than the cost of membranes from GE. Electrodialysis membranes are a small market right now and their costs are likely to drop if demand increases and economies of scale is approached. To investigate the effect of significant, but reasonable, reductions in membrane cost, we performed the PV-EDR optimization using a membrane cell pair cost of $20. For reference, if the previous optimized PV-EDR system cost was calculated with a membrane cell pair cost of $20 instead of $150, the system cost would be $15,360. However, lower cost cell pairs allows for more flexibility in the design of the system. The optimized PV-EDR design with the reduced membrane cost of $20 per cell pair is shown in Table 3.4 and only costs $11,717. Because of the reduced capital cost of the EDR cell pairs, the optimized size of the ED system was larger, resulting in a reduced daily average operating time of 8.6 hours. A comparison of the hours operated per day for the EDR system optimized for $150 cell pairs and the system optimized for $20 cell pairs is shown in Figure 3-6. The $20 per cell pair design has a shorter average operating time and a wider spread of actual daily operating times, reflecting the increased operating flexibility allowed by operating exclusively during daylight hours compared to the optimized design with $150 cell pairs. This larger ED system stack with shorter operating time and higher peak power has a power profile that is better matched to the solar power profile, which allows for a downsized PV array and battery bank.

When the capital cost of the electrical load is comparable to the cost of the PV

Design Variable	Symbol	Cost	Quantity
PV Area	A_{PV}	\$98/m^2	31 m^2
Battery Capacity	E_{batt}	\$150/kWh	5 kWh
Water Storage Volume	V_{tank}	\$110/m^3	10 m^3
# ED Cell Pairs	N_{CP}	\$20/cell pair	133 cell pairs
Stack Voltage	v_{EDR}	N/A	95 V
Batch Size	V_{batch}	N/A	0.68 m^3
Desalination rate	r_{desal}	N/A	1224 LPH
Daily operating time	t_{op}	N/A	8.6 hours
Peak power	P_{pk}	N/A	2360 W
Total Cost			**\$11,717**

Table 3.4: Optimized PV-EDR design variables with \$20 cell pairs and a total optimized system cost of \$11,717. Due to the lower cell pair cost, ED stack size could be larger, decreasing the daily average operating time and thus could take advantage of the cost reductions associated with a flexible operating schedule.

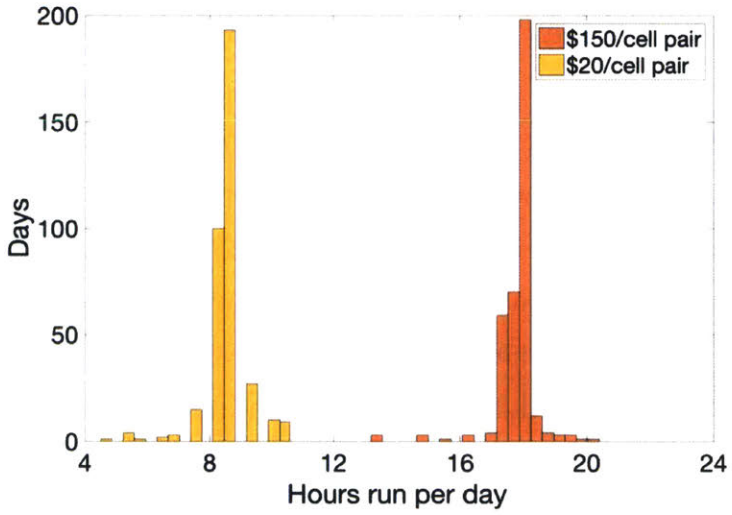

Figure 3-6: Histogram of daily operating hours of PV-EDR systems optimized with \$20 (average of 8.6 hours per day) and \$150 cell pair costs (17.7 hours per day).

power system, as was the case with the \$20 membrane cell pair system, there are dramatic reductions in the power system cost, and the PV-EDR system overall. This finding is consistent with the high sensitivity of total system capital cost to the cost of the membrane cell pairs described in the sensitivity analysis and motivates the development of lower-cost membranes, both through innovation and economies of

scale.

Furthermore, this case study of a PV-EDR system design with $20 cell pairs warrants investigation into operation flexibility and load sizing, which are two methods of shaping the electrical load to better match the time-variant solar power profile. Operation flexibility is the rescheduling of the operating time of an electrical load to occur during periods of high solar power output. Load sizing is the adjustment of the operating power level and average daily operating duration to better fit the diurnal nature of the solar power profile. Operation flexibility and load sizing are two generalized tools for PV-powered system design that can reduce the size and cost of the PV array and battery bank.

3.4.2 Flexible Operation

In Chapter 2, a theoretical reference system was introduced in which a PV subsystem powered a fixed load of 1 kW for a fixed schedule of 8 hours per day from 8AM to 4PM. For the remainder of this section, all analysis is conducted assuming this theoretical reference system and the same component costs from Table 2.2.

Here we investigate the power system cost reductions enabled by allowing the load operation schedule to shift in time according to the instantaneous solar irradiance available while maintaining an average operating time of 8 hours per day such that the system produces the same output as it would in a fixed operating schedule scenario. On long days with high solar irradiance, such as during the summer, the system would operate for longer and store the excess product to be collected on a day with low solar irradiance, such that the electrical load would not need to run at that time. Here it is assumed that the product is collected at a uniform rate throughout the year.

To determine the operation schedule that best matched the characteristic solar irradiance for the location, we calculated the highest cutoff value of solar irradiance for which the load should be turned on such that the load is run the same total amount of time over the course of the reference year compared to a load operating on a fixed, 8 hours per day operating schedule. The load profiles for the PV power system for a fixed and flexibly operated electrical load are shown in Figure 3-7.

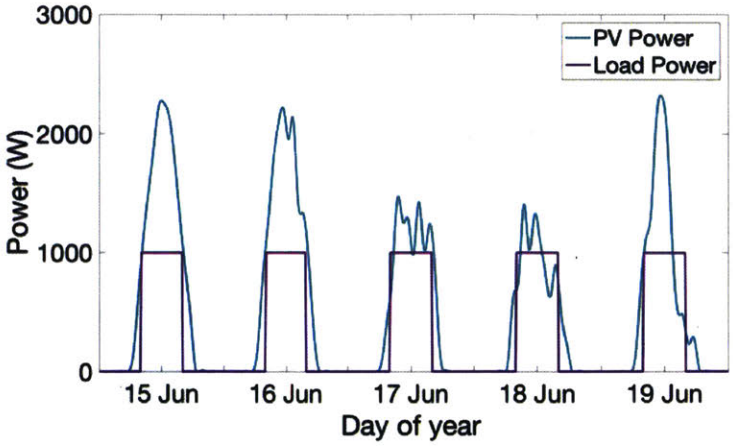

(a) Fixed operating schedule

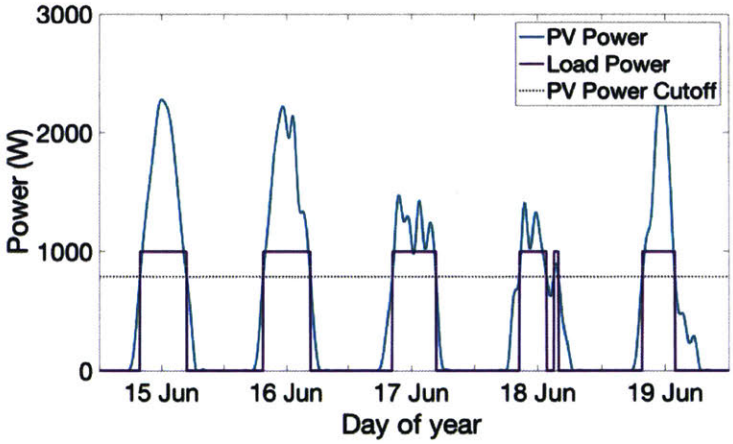

(b) Flexible operating schedule

Figure 3-7: PV and load power profiles for the reference system under fixed and flexible operation. (a) Reference system with fixed operating schedule (8AM-4PM at 1 kW) load power profile plotted against the power available from the solar power system over 5 days in June 2014; (b) Reference system with flexible operating schedule (8 hours daily average at 1 kW) load power profile and PV power cutoff beyond above which the load is turned on.

The frequency of number of hours operated per day for the reference year using the flexible operation schedule is represented in the histogram of Figure 3-8. On average, the system operates 8 hours per day, consistent with the fixed-schedule system. However, the spread shows the variability in days of abundant and scarce sunshine. The days with more than 8 hours of operation enable reliability and minimal operation

on days with little solar energy available.

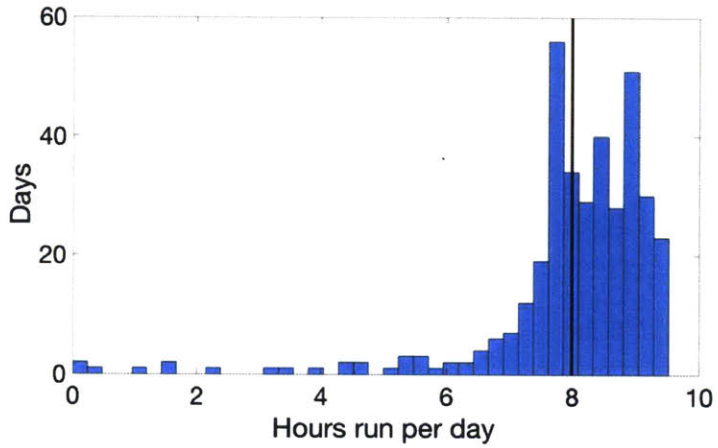

Figure 3-8: Histogram of hours operated per day for the flexibly operated reference system. The average is 8 hours, equivalent to the fixed operation schedule system, but the spread shows the variability in days of abundant and scarce sunshine. Long operation of 8+ hours on some days of the year enables reliability and minimal operation on the days of the year for which there is very low PV power output.

3.4.3 Load Sizing

Load sizing is the adjustment of the operating power and average duration of the load to better match the solar power profile. Certain processes, such as drip irrigation and municipal water supply, require a roughly constant energy to produce a set output over a day, but the sizing of the unit and the power at which it operates can be flexible over a range. The pumping system for irrigation or supplying a water tower, for example, could operate at high flow rate for a shorter period of time, or a low flow rate for a longer period of time. Here, the flexibly-operated reference system described above operates on average 8 hours per day, at 1 kW. Alternatively, another system of half the production capacity can operate at 0.5 kW and produce the same output in 16 hours. Or, another system twice the production capacity of the original can operate at 2 kW and produce the desired output in 4 hours. In each case, the energy used to run the system is the same, at an average 8 kWh per day.

A representation of the load power profile and PV power output for a PV-powered

system is shown in Figure 3-9. Load sizing is the adjustment of the load power profile to overlap more effectively with the typical PV power profile. In this analysis, I compare loads with different profiles but equivalent energy consumption (the area under the load power curve is kept constant).

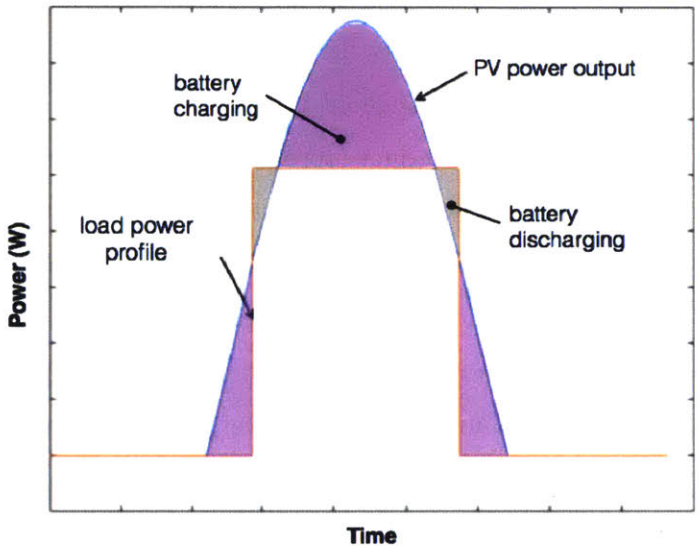

Figure 3-9: The overlaid load power profile and PV power profiles for a PV-powered system. Load sizing is the adjustment of the load power profile to better fit the characteristic PV profile, by adjusting the power level and duration of operating time.

3.4.4 Effects of Operation Flexibility and Load Sizing on the Reference System

The flexible operation schedule improves the overlap of the load power and PV power profiles. The storage requirement associated with variable PV area is shown in Figure 3-10a. For the same size PV array, the required energy storage is lower for the flexible operation case. Flexible operation also pushes the design towards a smaller PV array. However, the flexibly-operated design requires additional product storage for 100% output reliability, though this additional cost is not included in the power system cost shown in Figure 3-10b. Depending on the cost of product storage, flexible operation may be more or less favorable than fixed operation. In the flexible opera-

tion mode (Figure 3-7b and Figure 3-10), flexibility was maximized such that energy storage was minimized, and as a result, product storage was maximized. This meant that 82 hours worth of product needed to be stored to balance the fluctuations in annual solar availability to provide 100% output reliability. Therefore, flexible operation is cost-effective when the cost of product storage is less than the power system cost savings ($1,034 in this case) afforded by flexible operation. This analysis assumes a constant demand for the output throughout the annual cycle. If demand for output varies with solar irradiance, the product storage requirements and associated costs would be reduced, and flexible operation would become more cost-effective. This effect is expected with a product like desalinated drinking water, which would have a higher demand during sunnier, hotter times of the year.

To determine the effect of load sizing on power system cost, I calculated the lowest-cost combination of PV panels and batteries to meet the load power requirements for different load power profiles. For each load power profile, the energy consumption was held constant, while adjusting the constant power level and duration of operating time. The cost of the power system for designs with different lengths of average daily operating time (but equivalent energy consumption per unit output) are shown in Figure 3-11. The flexible-schedule systems have a lower cost than the fixed-schedule systems up to a 12-hour daily operating time, at which point flexible operation does not provide value because the system must always run at some point when there is no sunshine available.

The flexible operating schedule provides the greatest cost reductions around an average daily operating time of 5-8 hours, or corresponding power levels of 1-1.6 kW. This enables a power system cost reduction of 43% compared to a fixed-schedule system. It is important to note that higher-power electrical loads tend to have a higher associated capital cost than smaller, low-power loads, so there is a competing effect on the optimal electrical load size that may push the operating time to longer hours when the capital cost of the electrical load is considered. For example, if the capital cost of the electrical load is $4,000 for 0.5 kW, 16-hour operation, and $8,000 for 1 kW, 8-hour operation, the summed capital costs of the power system and electrical load

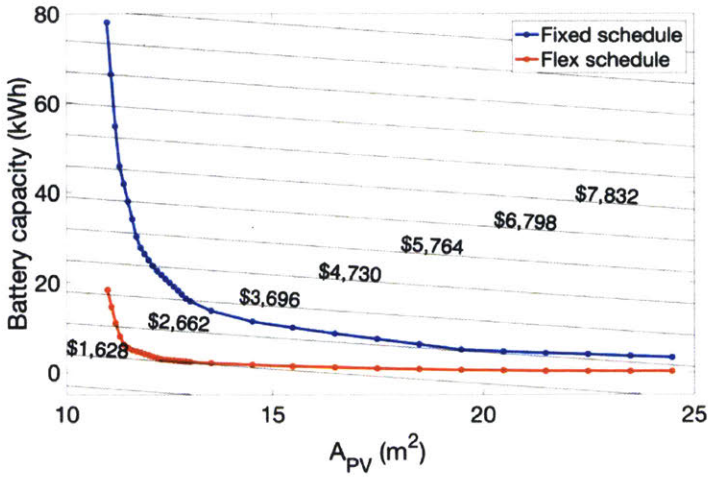

(a) Battery capacity vs PV area for fixed and flexible schedule operation

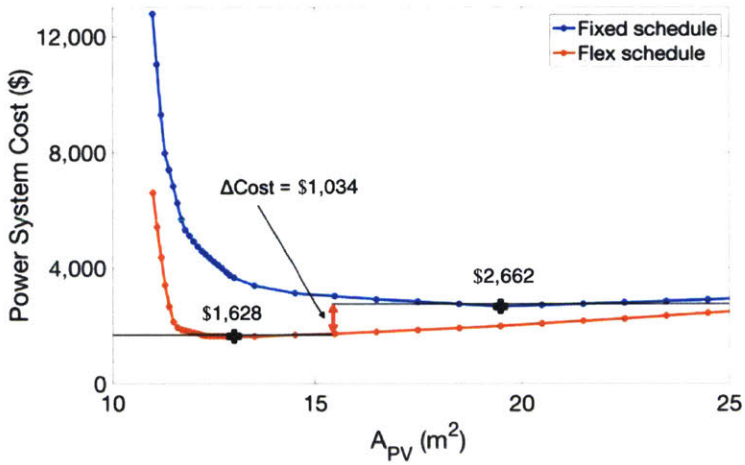

(b) Power system cost vs PV area for fixed and flexible schedule operation

Figure 3-10: Relationship between PV area, battery capacity and power system cost for fixed and flexible operation of the reference system. (a) The relationship between PV array size and storage requirement (represented here as battery capacity) for the reference system operating according to fixed and flexible schedules. The diagonal lines represent lines of constant power system cost and are determined by the ratio of energy storage and PV cost. (b) The relationship between PV array size and total power system cost (PV and batteries) for both fixed and flexible schedule designs. The black markers indicate the points of lowest power system cost ($2,662 for fixed operation and $1,628 for flexible operation).

would be $6,999 and $9,624, respectively. Because the capital cost of the electrical load is so high relative to the cost of the power system, the 0.5 kW, 16-hour design is

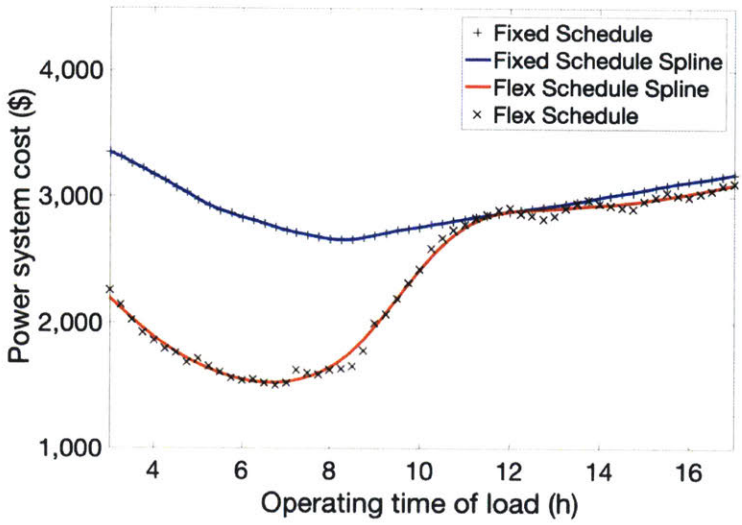

Figure 3-11: Lowest-cost power system (PV and batteries) for a flexibly-operated reference system with varying daily operating time/power levels. Each design consumes an average of 8 kWh per day, but the power at which it operates and the corresponding number of hours it runs per day varies along the x-axis. The flexible-schedule systems have a lower cost than the fixed-schedule systems up to a 12-hour daily operating time, at which point flexible operation does not provide value because the system must always run at some point when there is no sunshine available.

more cost-effective. Additionally, the flexible schedule system requires more product storage than the fixed schedule design, which may reduce the relative cost advantage of flexible operation depending on how much product storage costs.

These insights validate the observations made when the PV-EDR system design optimized with $20 cell pairs, specifically that the average daily operating time reduction from 17.7 hours per day to 8.6 hours per day also reduced the system capital cost. The PV-EDR design increased the ED stack size without large capital cost ramifications to have a greater water desalination production rate. This enabled the system to operate for 8.6 hours per day on average, close to the range of average daily operating times of 5-8 hours at which the cost reduction benefits are greatest when considering a flexible operating schedule. These insights therefore not only benefit the design of optimized PV-EDR systems, but also the design of any system whose operating schedule and load can be varied without affecting its quality or performance.

Chapter 4

Design and Field Testing

This chapter discusses the field testing and results of the PV-EDR system in the village of Chelluru, India. This village was chosen for a long-term field pilot study for many reasons. Chelluru has a Tata Projects on-grid RO system that has been operational for 8 years. From a research and field comparison standpoint, this enables us to establish a true side-by-side comparison of PV-EDR and RO performance over the long term. Furthermore, Chelluru as a village was willing to allow Tata Projects, our corporate and field partner in this research, to install an R&D project – our pilot PV-EDR system – in their village. In fact, the building that keeps the RO system had enough space to house an ED system so no additional protective housing structure would need to be arranged. Chelluru's current RO plant operator was willing to take on more responsibility to help run and maintain the PV-EDR system. Given the operator's successful 8-year track record and having worked closely with him a number of times, Tata Projects knows that the operator is reliable and trusts that he would follow instructions and would not knowingly interfere with an R&D project. Chelluru is also relatively close to the Tata Projects headquarters in Hyderabad compared to other villages under consideration, which was an important consideration for Tata Projects as their employees would need to access the system without too much inconvenience.

4.1 Experimental Setup

To collect real-time weather data to feed into the models to validate the field pilot test, a weather station was installed in the Tata Projects Water Development Center near Hyderabad, India. A Campbell Scientific LI200RX pyranometer was used to measure solar irradiance, and a HC2S3 temperature and relative humidity probe was used to measure the ambient temperature.

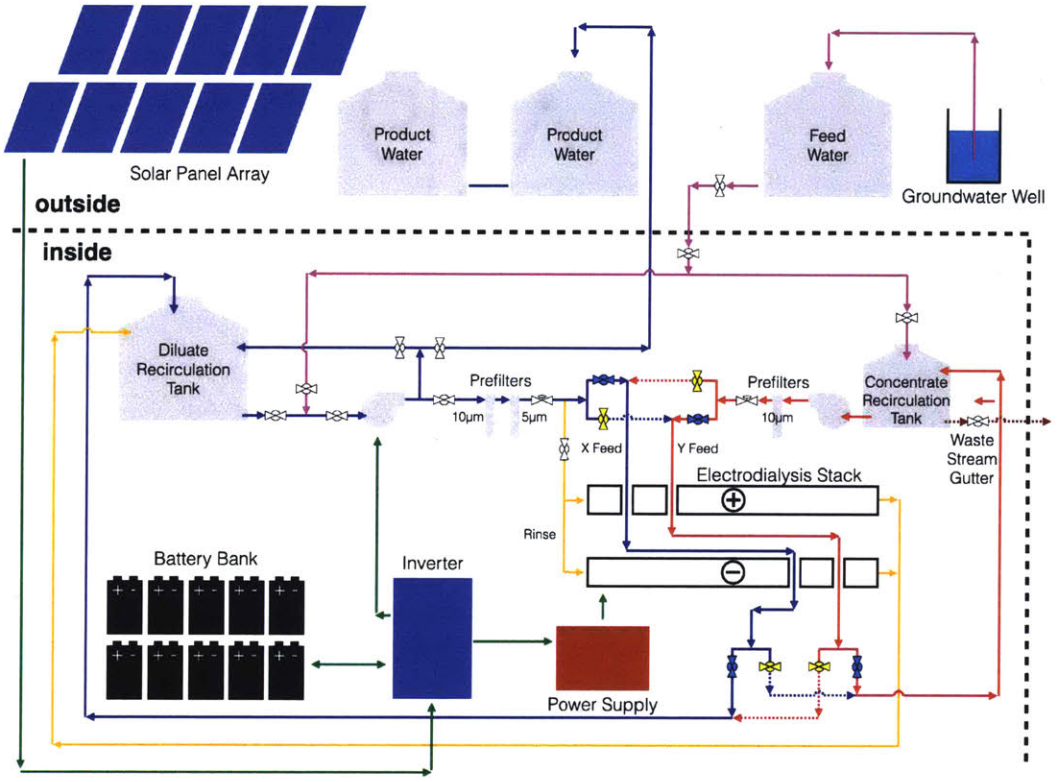

Figure 4-1: Detailed system layout of the pilot PV-EDR system installed in Chelluru.

The PV-EDR system was installed alongside an existing grid-connected RO system in Chelluru. The PV array was installed on the rooftop (Figure 4-2) while the EDR system, pumps, batteries and inverter were installed inside the small building housing the RO system. The inverter model is the UTL Alfa PCU, which is capable of measuring and exporting time-resolved data related to the PV power, battery status and load capacity. The full PV-EDR pilot system was assembled as detailed in Figure 4-1. Due to practical considerations not encompassed by our model and

Figure 4-2: Actual solar panels installed on the rooftop of the building housing the desalination system in Chelluru.

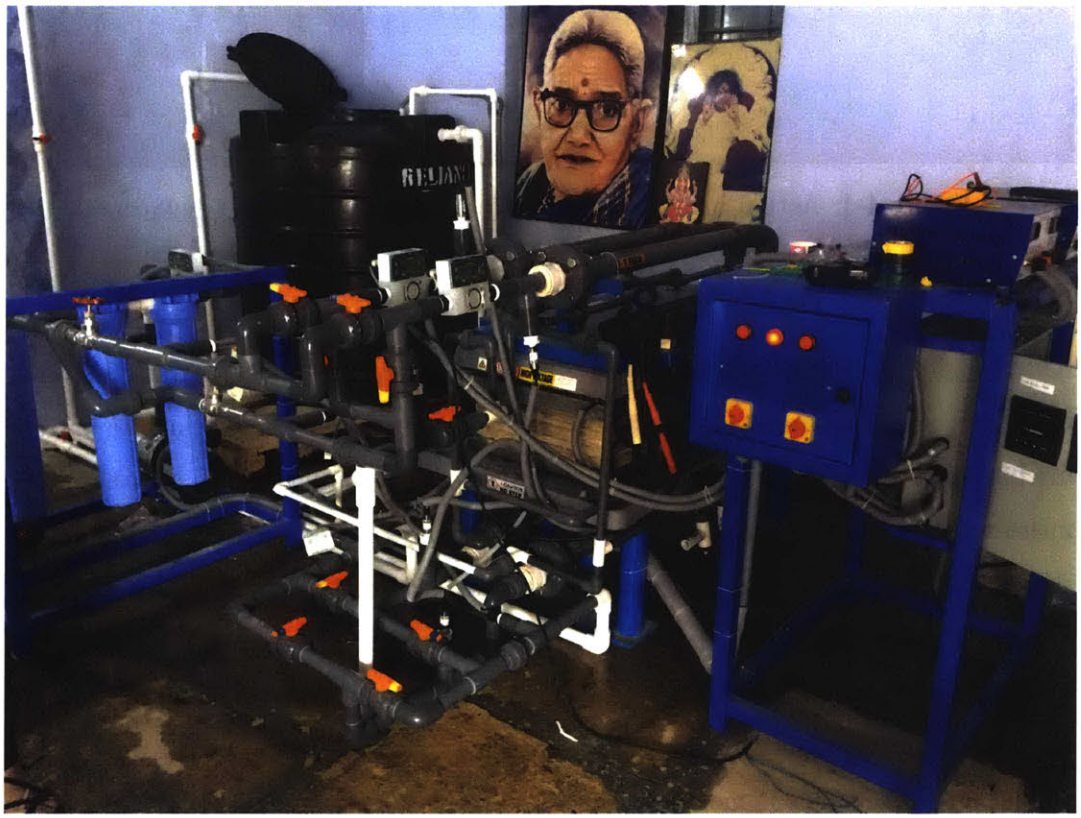

Figure 4-3: Actual electrodialysis reversal system installed in Chelluru.

adjustments to the model made post-installation, the experimental system deviated from the optimized system described in the previous section in the following ways:

Figure 4-4: Actual inverter (left) and batteries installed in Chelluru.

PV-EDR Model Modifications

After the design and installation of the Chelluru EDR system, an error was discovered in the power system code that miscalculated the energy used by EDR during a battery discharging state. While Equation 2.5 is only meant to be for charging, it had been mistakenly used for discharging as well, resulting in less energy discharge than there should have been. This error caused the Chelluru system to be undersized, and only capable of producing 7 m^3 of water per day rather than the expected 10 m^3. This error was corrected in the analyses presented in this thesis, but is a primary cause for the lower water production rates observed during village testing. For the purposes of validating the model, the model was adjusted to match the system that was actually installed in Chelluru.

PV-EDR System Component Composition

The composition of the experimental system varied in some respects to the optimized system due to practical constraints and limitations of what was actually available in India.

a. The GE ED stack is composed of two electrical stages which have four electrodes. However, it was modified to only use one electrical stage and therefore it effectively had two electrodes rather than four. Due to the architecture of the stack and the spacers, electrical stages could not be removed. The first electrical stage was not electrified and the water streams were routed through spacers and no membranes to minimize the pressure losses. The second electrical stage had a voltage applied and consisted of full sets of cell pairs as usual. Only the electrodes associated with the electrified stage were counted toward the pilot system capital cost.

b. The Kirloskar Wonder III pumps selected by the optimization were not corrosion-resistant, so Grundfos CM 3-3 pumps with similar flow and pressure characteristics and corrosion-resistant stainless steel (SS316) construction were substituted. These pumps cost $239 each compared to the Kirloskar Wonder III cost of $44 each.

c. A power supply was used to convert the AC voltage output of the inverter to a DC voltage that could be applied to the stack.

d. The inverter used was the UTL Alfa PCU which was selected retroactively by the supplier who provided the solar panels and batteries. The cost of the inverter was not considered in the optimization.

e. Using the original model with the battery discharging error described above in PV-EDR Model Modifications, the initial cost-optimized system had a battery bank of 15.5 kWh with a discharge depth of 50%. In the installed system, this translated to ten 12 V, 135 Ah lead-acid batteries, or 16.2 kWh, with a discharge depth of 50%. These batteries were selected by the supplier to provide the desired amount of energy and to be consistent with the rated 120V DC input for the inverter. While a 16.2 kWh battery bank was installed in the village, the optimized system with the battery discharge model correction should have a battery bank of 22 kWh and was discussed

in Chapter 3.

f. Finally, the system also consisted of several components that were not considered in the optimization but add to the actual total capital cost. These include recirculation tanks, piping, valves, cartridge filters for pre-filtration, PV mounting structures, wiring and grounding elements.

PV-EDR System Operation

a. The simulation used to design the village PV-EDR system did not consider the recirculation tank filling and draining time and associated pumping power. The filling and draining added approximately 20 minutes to each batch, during which time one 410 W pump was running.

b. The PV-EDR system was manually operated. This consisted of turning on and off the pumps and the power supply and switching the valves to apply the reversal of streams for EDR.

c. On Day 4 of the 7-day testing period, significant scaling was observed within the stack because of precipitation of dissolved salts in the concentrate stream. Day 5 was spent opening up the stack to wash the precipitated salt from each individual membrane and spacer. To alleviate this scaling issue, the recovery ratio was reduced from 90% to 80% by approximately doubling the brine volume for the remainder of the test, Days 6 and 7.

c. During testing on Day 4 (April 23), it was observed that the flow rate into the stack had decreased dramatically and upon inspection, discovered that scale formations had been accumulating in the ED stack over the course of the first few days of testing. This appeared to have occurred due to high concentrations of calcium carbonate and calcium sulfate, causing the salts to precipitate out of solution. There was a 23-hour gap between batches during which the ED stack was opened up and rinsed to clean the membranes of the scale formations. To prevent this issue from occurring again, the recovery ratio was decreased to approximately 80%, approximately doubling the brine volume fro the remainder of the test, Days 6 and 7.

4.2 Experimental Procedure

The PV-EDR system was run in the village from 4:30PM on April 19 to 4:30PM on April 26, 2017, for a total period of 7 days. A single EDR batch was comprised of a complete cycle of filling the recirculation tanks, desalinating the water, and emptying the recirculation tanks. The filling phase consisted of pumping water from the feed water storage tank to fill the diluate and brine recirculation tanks; desalinating consisted of circulating the water through the ED stack while applying the desired voltage until the average salinity in the diluate tank was measured to be 300 mg/L or less; and emptying consisted of draining the brine water into the village gutter and pumping the diluate water into product water holding tanks.

Another irregularity during the week-long test was the presence of several gaps in the data recorded by the inverter, for minutes to hours at a time. We expect this was due to a faulty condition in the inverter datalogging process. Because this missing data could not be recovered, there are several gaps in the experimental data presented in the following sections.

4.3 Results and Discussion: Comparison of the Modeled and Measured Performance

4.3.1 EDR Load Power

At the Chelluru test site, the load power was measured through the inverter, and the pumping power was verified by measuring the AC current to each pump with a multimeter. The power profiles of filling and emptying the recirculation tanks before and after each batch, respectively, were added into the model. In order to compare the power profile during the desalination phase, the simulated power draw during that period was plotted against the average experimental power draw and the range of a single standard deviation over the course of 46 batches. The average power draw profile over the course of the desalination phase observed in the experiments exceeded

that of the simulated power draw profile during the first half of the batch and dropped below by the end of the batch. On average, the energy consumption was greater than expected, which would decrease the system's overall production capacity, but the model closely predicts performance within 13.5% and almost perfectly matches the expected batch duration of 60 minutes.

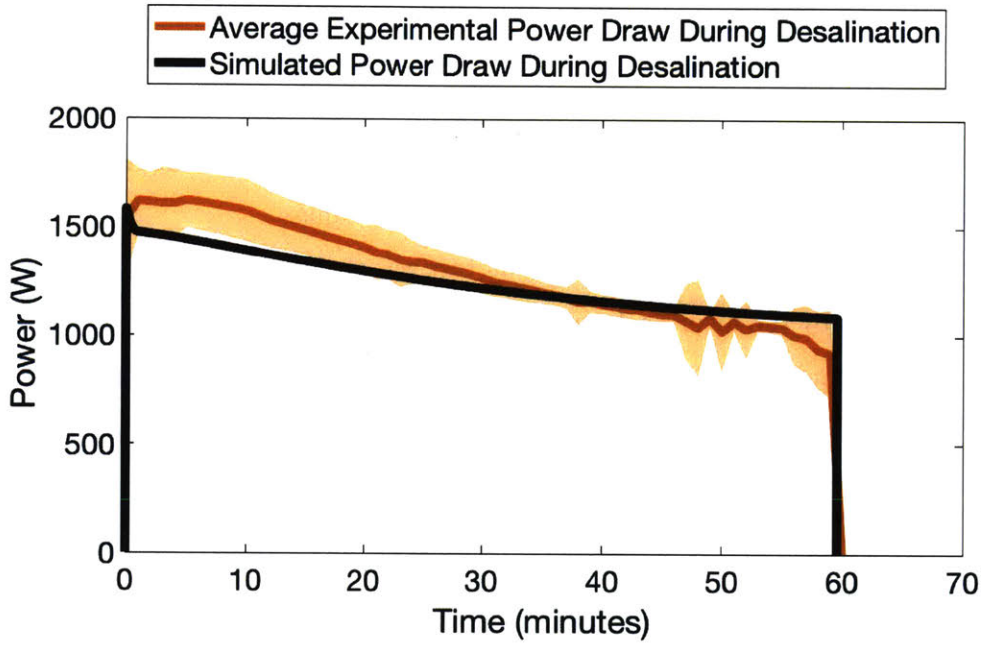

Figure 4-5: Simulated power draw profile during the desalination phase of a single batch (black) compared to the average of 46 measured batch power profiles (orange). In addition to the average, the range of one standard deviation above and below the average was also included (orange). Experimental desalination phase duration averaged 60 minutes as predicted, though most durations ranged 45-80 minutes, with the extremes being 32 and 115 minutes. The recovery ratio was changed from 90% to 80% for the last two days of testing, which may have affected the results shown here.

An inconsistency observed during the experiments, was that while the desalination phase duration averaged 60 minutes, it varied from batch to batch, sometimes widely, ranging from 32 to 115 minutes at the extremes, though most were within the 45-80 minute range. The scaling issue could explain a few of the longest duration batches, as the flow rate, and thus the desalination rate, decreased dramatically as the stack became clogged with salt. Additionally, while there was some variation in batch

volume during testing, these differences do not fully account for the full range of variations in batch duration that we observed.

A comparison between the modeled and measured power profiles over the course of a single day (April 20, 2017) are plotted in Figure 4-6. The modeled power profiles consist of 20 minutes of draining and refilling the recirculation tanks with one 410 W pump on, followed by a 60 minute-long EDR batch with two 410 W pumps running and the voltage applied across the stack, decreasing in power over time. Due to the data collection failures, data from a number of the batches that were run are missing, including two batches in the morning of April 20.

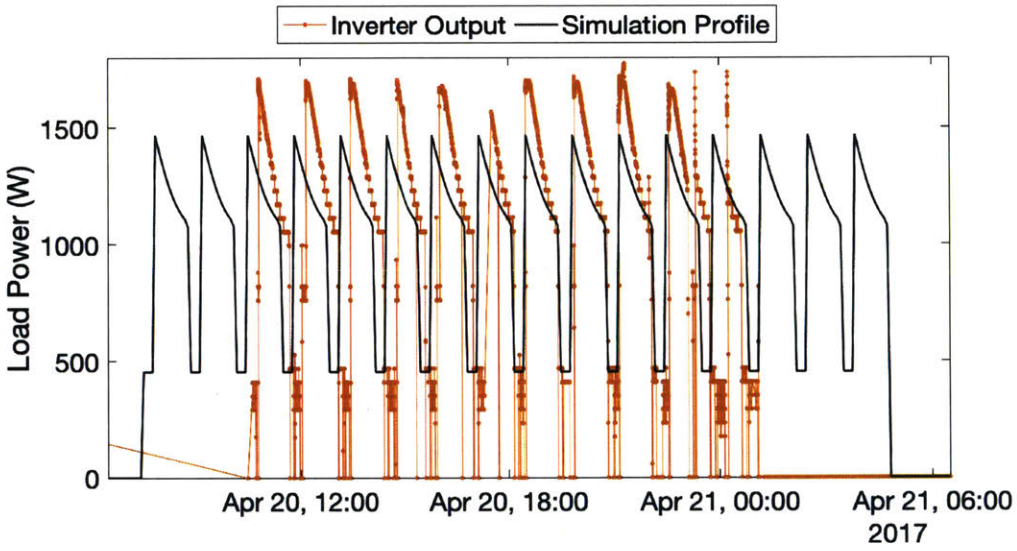

Figure 4-6: EDR load power. Comparison between the power output data collected from the inverter in April 2017 (orange) and the expected power profile based on the simulation model over the course of 2014 (black).

The power load measured by the inverter during the desalination phase was higher than anticipated through the model, particularly at the beginning of each batch, though the experimental power draw matched the model well and was sometimes less than the model near the end of each batch. Because the pumping power measured by the inverter was validated through separately measuring the current to the pumps, the discrepancy is suspected to be caused somewhere in the power transfer to the

ED stack. Manual measurements of the stack voltage and current into the stack were made periodically throughout a few batches. These measurements indicated that the actual power consumption according to the manual measurements was in better agreement with the model than the data collected from the inverter. This may indicate that the power supply used to supply the DC voltage to the ED stack has a substantially lower efficiency at high power outputs than at lower power outputs, due to heat for example. This could explain why the modeled and measured values differ greatly at the beginning of a batch but converge near the end. Another potential source of error is the fact that the ED model is based on behavior with dissolved sodium chloride (NaCl), while the actual groundwater of Chelluru has a much more complex composition.

4.3.2 PV Panel Output

The solar power produced by the PV array was measured at the Chelluru test site through the UTL Alfa PCU inverter, and the solar irradiance was measured at the Tata Projects Water Development Center manufacturing facility (approximately 60 km west of Chelluru) and used to calculate a modeled PV power output based on the 40 m^2 of panels of the pilot system according to the method described in the PV Power System Behavior section in Chapter 2. A comparison of the measured PV power output from the pilot system inverter, the PV power output used in our simulation to design the system (based on semi-empirical 2014 weather data), and the modeled PV array power output (using the measured 2017 weather data) is shown in Figure 4-7.

The 2014 semi-empirical data and the measured 2017 data from the weather station are very similar. Though it is not an indication of long-term agreement, it does indicate that the simulation results using the 2014 data should be similar to those based on the 2017 data.

The power production measured by the inverter was in good agreement with the 2017 weather data as well. However, it was observed that while there was a load running, the solar panel current would vary with the power drawn by the load, which

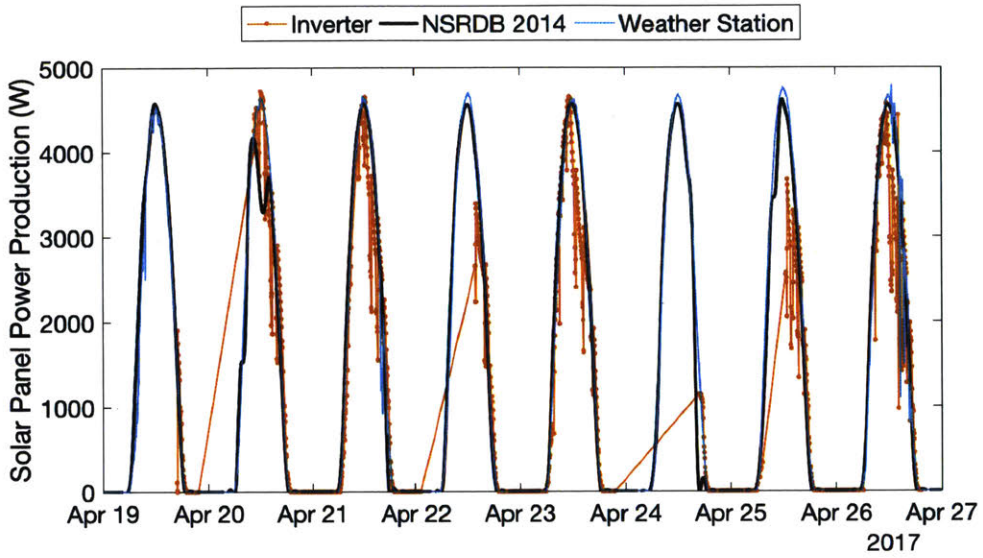

Figure 4-7: Comparison between the solar panel power production data collected from the inverter in April 2017 (orange), the simulation model based on the NSRDB 2014 weather data (black), and the model prediction using the weather data collected from the installed weather station (blue).

may be an artifact of how it is measured and account for the oscillations in inverter-measured PV power output. As mentioned previously, there were periods when the data from the inverter was not recorded, which account for the large gaps in portions of the figure. Despite this, the inverter measurements seem to reproduce actual solar panel output reasonably well.

4.3.3 Battery Energy Stored

The inverter did not directly output the battery energy levels. However, an estimation of the energy stored in the battery for the 7-day test was calculated using the battery voltage, charging, and discharging current reported by inverter. The relative change in energy between time increments was calculated according to

$$\Delta E_{stored}(t) = \Delta t \cdot v_{batt}(i_{chg} - i_{dsg}), \tag{4.1}$$

where ΔE_{stored} is the change in stored energy over the time increment, Δt is the time

interval between samples (approximately 1.94 seconds), v_{batt} is the battery voltage, i_{chg} is the battery charging current, and i_{dsg} is the battery discharge current. Whenever the battery voltage indicated that the batteries were fully charged (v_{batt} âĽě 144 V), ΔE_{stored} was assumed zero. Because the data had gaps due to inverter data recording failures, the absolute positions of the battery energy curves were shifted such that their maxima were located at the full energy state of 16.2 kWh. These curves are plotted against the battery energy calculated from the simulated EDR power profile and simulated PV power profiles described in the previous sections according to Equations 2.5 and 2.6 (Figure 4-8).

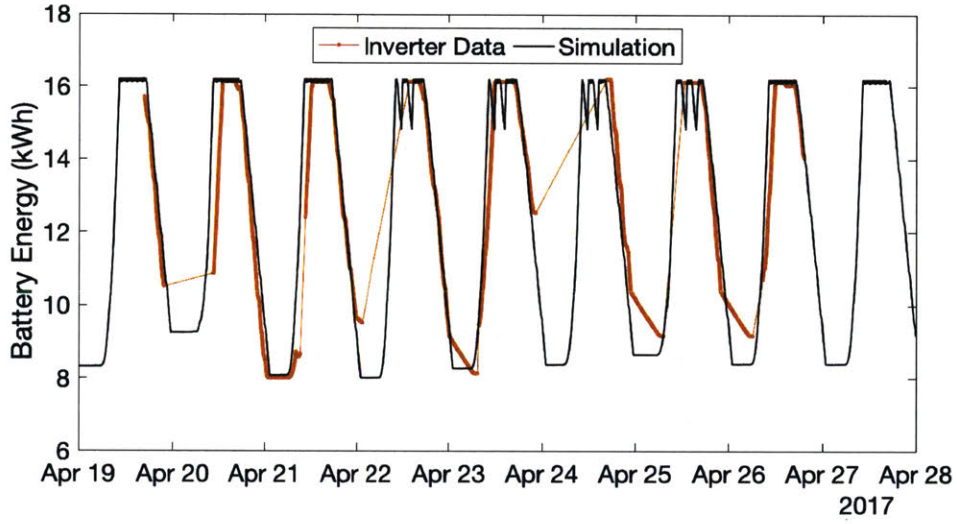

Figure 4-8: Comparison between the battery energy calculated based on data collected from the inverter in April 2017 (orange) and the expected battery energy based on the simulation model over the course of 2014 (black).

Due to inverter data collection failures, there was only one night over the course of the week-long test during which the batteries could be verified to be depleted to the specified discharge depth of 50%. However, the rates of charging and discharging of the batteries is a very close match to the model. This was expected because of the good agreement between model and experiment of both the load power and PV panel power output.

Chapter 5

Conclusions and Future Work

In this research, I aimed to identify the lowest-capital cost village-scale photovoltaic-powered electrodialysis desalination system for rural India based on current component prices and performance. I investigated the parametric relationships that govern the characteristics of the electrodialysis process and the photovoltaic power systems and created a model to predict a PV-EDR system's performance. Through optimization, I was able to find that the cost of the optimal system was $23,420, a 42% reduction from the $40,138 cost of a PV-EDR system designed using convention methods of sequentially designing the load and then the power system. I then physically built the PV-EDR system, installed it in the village of Chelluru in India, and personally ran a week-long trial to collect initial data and results. With the exception of a few practical points not considered in the model, the results match the PV-EDR system performance model quite well, including solar irradiance, batch power and battery energy levels.

In this thesis, I first discuss the variables and equations governing the behavior of the electrodialysis process and the photovoltaic power system. This understanding allowed me to develop a simulation model to predict the cost and performance of a system using the interactions between the electrodialysis and photovoltaic power subsystems. The model developed is generalized to take inputs of local conditions such as feed water salinity, desired product water salinity, water demand profile, irradiance data and temperature data. It will then evaluate the performance of a

user-defined PV-EDR system design and output the system's cost and reliability. By coupling the simulation model to a particle swarm optimization algorithm, an optimal design for the given input parameters can be found. In doing so, I found a near cost-optimal design configuration for a PV-EDR system designed for the median village in India, and focusing on Chelluru specifically by using its local solar irradiance and temperature data as well as the local groundwater salinity. This design consists of an electrodialysis system of a GE ED stack with 62 cell pairs with an applied potential of 45 V and running batch sizes of 0.42 m^3 and water storage tank of 10 m^3, and a photovoltaic power system with 57.5 m^2 of PV panels and 15.5 kWh of batteries. This design runs for an average of 17.7 hours per day to provide the daily water requirement of 10 m^3. The production rate of water is low because there are relatively few cell pairs in the ED stack, a result of the cell pair cost being so high relative to other components. Therefore, by minimizing the number of cell pairs, the cost of the system could also be reduced. This optimized design (Design A) was compared to a PV-EDR system designed using conventional methods of deciding the desired daily operating time, followed by designing the load to meet that time, followed by designing a PV power system with two days of battery backup (Design B). As expected, the cost of Design A was significantly lower at $23,420 compared to $40,138 for Design B.

Other optimal designs were also examined to investigate the parametric sensitivities of system capital cost to output reliability, feed and product water salinities, and individual component costs. It was found that relaxing the required output reliability from 100% to 98% reduced the capital cost of the system by approximately 5.7%, while reducing the reliability to 10% only reduced the capital cost of the system by approximately 10.3%, a marginal improvement. This indicates that a handful of days during the least sunny time of the year disproportionately drive up the system capital cost.

The high sensitivity of the optimal PV-EDR system design to the cost of membrane cell pairs prompted an investigation into how the PV-EDR system would change with $20 cell pairs instead of $150. It was found that the ED stack was much larger compared to the optimal design with $150 cell pairs. This enabled the system to pro-

duce desalinated water faster and operate on average for fewer hours per day. Most notably, the cost reduction enabled by the increased operation schedule flexibility was significant, even after accounting for the fact that the membrane costs differed.

Based on these results, the benefits of flexible schedule operation and load sizing were also examined. A load running on a flexible schedule, compared to one running on a fixed schedule, will see system cost reductions by better matching the load to the availability of solar irradiance. These benefits were found to be greatest if the daily operation time of the load is less than 12 hours, specifically 5-8 hours, enabling more flexibility during daylight hours. This flexibility enables a system to run the load longer during high irradiance days and shorter during low irradiance days. However, flexible operation requires product storage to meet a constant product demand over the annual cycle, so the cost of storage should taken into account. Load sizing can also reduce system cost through adjusting the system capacity, and lower power systems with slower production rates typically have lower capital costs. This reduction in load-related capital costs must be balanced and reconciled properly with the flexible schedule power system cost reductions of operating for less than 12 hours.

The pilot PV-EDR system was installed in Chelluru in January 2017. For a 7-day testing period in April 2017, the PV-EDR system model closely predicted the performance of the pilot system. This period coincided with the sunniest time of the year. We are currently arranging for a yearlong evaluation period to compare the accuracy of our model over the full irradiance cycle encompassing different seasons. Doing so will also be important for understanding the long-term performance of PV-EDR in the field since it is not currently well understood. Furthermore, it is expected that if water demand varies with solar irradiance, as might be expected with water demand increasing during hotter months and decreasing during cooler months, the energy and water buffering requirements would be reduced, which would further drive down the cost of the PV-EDR system. In this analysis, a constant water demand was assumed over the course of the year, because of a lack of seasonal water usage data for the region. The desalination system installed in Chelluru now has a sensor to track water withdrawal, and the data will be used in future work to more accurately

simulate future PV-EDR designs, and likely contribute to cost reductions in the energy and water storage elements. If validated, this model will be useful for evaluating the performance and economic feasibility of PV-EDR systems in other locations in India and around the world.

In conjunction to the yearlong evaluation period, we are coordinating with Tata Projects to conduct a blind test of the ED product water from our system and the RO product from the grid-connected system. It was brought to our attention that the people of Chelluru and other places that have access to clean drinking water are accustomed to water with salinity 70 mg/L or less. While the salt in the water cannot be tasted below 500 mg/L, there may still be some kind of aesthetic differences between water at 300 mg/L and 70 mg/L, which the blind test will aim to confirm or deny in Chelluru. If confirmed and the 300 mg/L ED product water from our system is undesirable compared to the 70 mg/L RO product water, there are a few options for how to proceed. We could determine the ED operating characteristics necessary to produce water at a salinity the people will accept. Alternatively, the ED product water could be trucked to another location where the people are not accustomed to very low salinities and would accept our water, the water could be used for agriculture, or it can act as feed water to the village's RO system.

Potential areas for future work include:

- *Cost modeling of the full desalination system installation process:*
  In this thesis we modeled the cost of the major PV-EDR system components, but there are many other costs to consider. Aside from the minor system components like piping, ball valves and cartridge filters, there are costs associated with shipping the components to the village, erecting a housing structure, evaluating the local groundwater, etc. These all contribute to the full cost of the system.

- *Investigate minor energy or water interventions*
  The sensitivity analysis conducted found that relaxing the output reliability from 100% to 98% reduced the capital cost of the system by approximately

5.7%. The drop in reliability of a lower cost system could be removed by supplementing the power system with an input such as a diesel generator or grid connection in locations where the grid is operational for a small amount of time. The water supply could also be supplemented with water that is trucked in locally during the times of year where the PV-EDR system would otherwise not meet demand. Supplementing the system from an energy or water perspective can result in large cost reductions.

- *Incorporating variable voltage operation:*

  Constant voltage operation is beneficial for its simplicity, but there is opportunity to run the ED process at a voltage such that the maximum current density is applied at all times or even such that the power applied to the stack roughly matches the solar irradiance profile. The exact benefits of this for an off-grid system are not quantified, though more power would be consumed in less time per batch. Operating for fewer hours per day could lead to potential benefits from a flexible operation schedule.

- *Water demand modeling*

  The ability to model demand and time-resolved water collection data as a function of local community population, temperature, rainfall, proximity to other water sources, etc. is critical for more accurately simulating future PV-EDR and other desalination systems. Doing so would create a more accurate simulation model and demonstrate whether previous demand assumptions were too conservative or aggressive. The sensors installed in Chelluru to track the community's water withdrawal is one of the first steps taken towards achieving this goal.

Bibliography

[1] UNICEF and World Health Organization. Progress on sanitation and drinking water. 2015 Update and MDG Assessment, 2015. WHO Press. Geneva, Switzerland.

[2] WHO / UNICEF Joint Monitoring Programme for Water Supply and Sanitation. Improved and unimproved water sources and sanitation facilities. Available from `https://www.wssinfo.org/definitions-methods/watsan-categories/`. (Accessed 02/20/17).

[3] Office of the Registrar General and Census Commissioner, India. Censusindia.gov: Population Enumeration Data (Final Population): A-1 Number of Villages, Towns, Households, Population and Area (Accessed 02/20/17).

[4] Central Ground Water Board. Ground Water Quality in Shallow Aquifers of India. Technical report, Government of India, 2010.

[5] Wright, N. (2014). Justification of Village Scale Photovoltaic Powered Electrodialysis Desalination Systems for Rural India. Master's thesis, Massachusetts Institute of Technology, Cambridge, Massachusetts.

[6] Bureau of Indian Standards. Drinking Water - Specification (Second Revision: IS 10500). ISO 10500, 2012.

[7] Nataraja C. B. Personal Conversation with Nataraja C. B., Tata Projects Water Purification Plant Development Center, Secunderabad, India. August 2016.

[8] Open Government Data Platform India. Data.gov.in: Progress Report of Village Electrification as on May 2015. Available from https://data.gov.in/visualize/?inst=e66ecc8f79fbde7c078b6c5f497efb80. (Accessed February 28, 2017).

[9] C. Chandramouli. Census of India 2011 - Household Amenities and Assets: Source of Lighting. Technical report, Government of India, 2012.

[10] National Renewable Energy Laboratory. India Solar Resource - Global Horizontal Irradiance. Available from http://www.nrel.gov/international/images/india_ghi_annual.jpg. (Accessed March 14, 2017).

[11] Nataraja C. B. (personal communication, May 27, 2016).

[12] Wright, N. C., and Amos G. Winter, V., 2014. âĂIJJustification for community-scale photovoltaic powered electrodialysis desalination systems for inland rural villages in IndiaâĂİ. Desalination, 352, pp. 82âĂŞ91.

[13] Prashant Mehta. "Impending water crisis in India and comparing clean water standards among developing and developed nations." Scholars Research Library, Archives of Applied Science Research, 2012. Available from http://www.scholarsresearchlibrary.com/articles/impending-water-crisis-in-india-and-comparing-clean-water-standards-among-develop pdf. (Accessed May 15, 2017).

[14] Keller, A., Sakthivadivel, R., Seckler, D. "Research Report 39: Water Scarcity and the Role of Storage in Development." International Water Management Institute.

[15] Chinnasamy, P., Agoramoorthy, G. "Groundwater Storage and Depletion Trends in Tamil Nadu State, India." Water Resources Management, May 2015, Volume 29, Issue 7, pp. 2139-2152.

[16] Anthony Lopez, Billy Roberts, India Solar Resource âĂŤ Direct Normal Irradiance, National Renewable Energy Laboratory, 2013.

[17] National Renewable Energy Laboratory, India Solar Resource âĂŤ Direct Normal Irradiance, http://www.nrel.gov/international/images/india_dni_annual.jpg. (Accessed May 9, 2014, as cited in Wright, 2014).

[18] Bloomberg New Energy Finance. "The Cost Landscape of Solar and Wind" (2015). Bloomberg database, January 2015.

[19] M. E. Glavin and W. G. Hurley, "Optimisation of a photovoltaic battery ultracapacitor hybrid energy storage system," Solar Energy, pp. 3009-3020, October 2012.

[20] C. Olcan, "Multi-objective analytical model for optimal sizing of stand-alone photovoltaic water pumping systems," Energy Conversion and Management, vol. 100, pp. 358-369, May 2015.

[21] Y. Bakelli, A. H. Arab and B. Azoui, "Optimal sizing of photovoltaic pumping system with water tank storage using LPSP concept," Solar Energy, vol. 85, pp. 288-294, December 2011.

[22] . Smaoui, A. Abdelkafi and L. Krichen, "Optimal sizing of stand-alone photovoltaic/wind/hydrogen hybrid system supplying a desalination unit," Solar Energy, vol. 120, pp. 263-276, 2015.

[23] A. H. Habib, V. R. Disfani, J. Kleissl and R. A. de Callafon, "Optimal switchable load sizing and scheduling for standalone renewable energy systems," Solar Energy, vol. 144, pp. 707-720, 2017.

[24] L. B. Jaramillo and A. Weidlich, "Optimal microgrid scheduling with peak load reduction involving an electrolyzer and flexible loads," Applied Energy, vol. 169, pp. 857-865, 2016.

[25] Ortiz, J., ExpÃşsito, E., Gallud, F., Garcia-Garcia, V., Montiel, V., and Aldaz, A., 2006. âĂIJPhotovoltaic electrodialysis system for brackish water desalination: Modeling of global processâĂİ. Journal of Membrane Science, 274 (1-2), Apr., pp. 138âĂŞ149.

[26] Adiga, M. R., Adhikary, S., Narayanan, P., Harkare, W., Gomkale, S., and Govindan, K., 1987. âĂIJPerformance Analysis of Photovoltaic Electrodialysis Desalination Plant at Tanote in Thar DesertâĂİ. Desalination, 67, pp. 59âĂŞ66.

[27] Kuroda, O., Takahashi, S., Wakamatsu, K., Itoh, S., Kubota, S., Kikuchi, K., Eguchi, Y., Ikenaga, Y., Sohma, N., Nishinoiri, K, 1987. "An Electrodialysis Sea Water Desalination System Powered By Photovoltaic Cells". Desalination, 65, pp. 161-169.

[28] N. Soma, F. Kanenobu, S. Inoue and O. Kuroda, "The practical operation of photovoltaic desalination systems," International Journal of Solar Energy, vol. 13, pp. 97-109, 1992.

[29] Bilton, A. (2006). A Modular Design Architecture for Application to Community-Scale Photovoltaic-Powered Reverse Osmosis Systems. Doctor of Philosophy thesis, Massachusetts Institute of Technology, Cambridge, Massachusetts.

[30] Bilton, A., Dubowsky, S. "Modular Design of Community-Scale Photovoltaic Reverse Osmosis Systems Under Uncertainty." in Proceedings of the ASME, 40th Design Automation Conference, 2014.

[31] A. Bilton, "A Modular Design Architecture for Application to Community-Scale Photovoltaic-Powered Reverse Osmosis Systems," Cambridge, 2006.

[32] Amy M. Bilton & Leah C. Kelley (2015) Design of power systems for reverse osmosis desalination in remote communities, Desalination and Water Treatment, 55:10, 2868-2883, DOI: 10.1080/19443994.2014.940641

[33] General Electric Water & Process Technologies (1998). GE Aquamite EDR Systems Fact Sheet. Retrieved from the GE Water & Process Technologies Document Library website `https://www.gewater.com/kcpguest/document-library.do`. (Accessed May 19, 2017).

[34] Datanet India Pvt. Ltd. Indiastat.com: Revealing India-Statistically: State-wise Distribution of Inhabited Villages According to Population of India (Accessed November 10, 2013, as cited in Wright, 2014).

[35] Peter H. Gleick, Basic water requirements for human activities:meeting basic needs, Water Int. 21 (2) (June 1996) 83âĂŞ92.

[36] Natasha C. Wright, Sahil R. Shah, Amos G. Winter, V. "Validated Model of the Desalination and Pumping Energetic Requirements of Brackish Water Electrodialysis at Multiple Size Scales" (In Preparation).

[37] Wright, N.C., Van de Zande, G.D., and Winter, A., Design of a Village-Scale PV Powered Electrodialysis Reversal System for Brackish Water Desalination in India. The International Desalination Association World Congress on Desalination and Water Reuse 2015. San Diego, CA, USA.

[38] J. M. Ortiz, J. a. Sotoca, E. Exposito, F. Gallud, V. Garca-Garca, V. Montiel, and a. Aldaz, "Brackish water desalination by electrodialysis: Batch recirculation operation modeling," Journal of Membrane Science, vol. 252, no. 1-2, pp. 65-75, 2005.

[39] H. Strathmann, Electrodialysis, a mature technology with a multitude of new applications," Desalination, vol. 264, no. 3, pp. 268-288, 2010.

[40] Y. Tanaka, Ion Exchange Membrane Electrodialysis: Fundamentals, Desalination, Separation. Nova Science Publishers, 2010.

[41] General Electric Water & Process Technologies (1998). New High-Performance Spacer in Electrodialysis Reversal (EDR) Systems. Retrieved from the GE Water & Process Technologies Document Library website `https://www.gewater.com/kcpguest/document-library.do`. (Accessed October 3, 2016).

[42] National Renewable Energy Laboratory (NREL). Latitude: 17.84, Longitude: 79.35, Country: India, Year: 2014. Available from `https://maps.nrel.gov/nsrdb-viewer/`. (Accessed September 20, 2016).

[43] "Suniva Optimus Series Monocrystalline Solar Modules," [Online]. Available from https://www.wholesalesolar.com/cms/suniva-suniva-opt330-72-4-100-silver-mono-solar-panel-specs-1610309543.pdf. (Accessed May 20, 2016).

[44] N. Pearsall, Ed., The Performance of Photovoltaic (PV) Systems: Modeling, Measurement and Assessment, vol. 105, Woodhead Publishing, 2017.

[45] B. S. Borowy and Z. M. Salameh, "Methodology for Optimally Sizing the Combination of a Battery Bank and PV Array in a Wind/PV Hybrid System," IEEE Transactions on Energy Conversion, vol. 11, no. 2, pp. 367-375, 1996.

[46] Nilesh S. Shrikhande. Personal Conversation with Nilesh S. Shrikhande, Tata Power Solar, Bangalore, India. July 2016.

[47] R. N. Chapman, Sizing Handbook for Stand-Alone Photovoltaic/Storage Systems, Albuquerque, NM: Sandia National Laboratories, 1987.

[48] Amy Rose, Andrew Campanella, Reja Amatya, and Robert Stoner (2015). Solar Power Applications in the Developing World. January. The MIT Future of Solar Energy Study Working Paper.

[49] Private Participation in Renewable Energy Database: Solar, World Bank (2013). Available from http://ppi-re.worldbank.org/snapshots/technology/solar#regional-breakdown. (December 5, 2016).

[50] General Electric Water & Process Technologies, 2014. Supplier quotations for ion exchange membranes. Westborough, MA.

[51] J. Kennedy and R. Eberhart, "Particle Swarm Optimization," in Proceedings of the IEEE International Conference on Neural Networks, Perth, 1995.

[52] J.H. Lienhard V, A. Bilton, M.A. Antar, G. Zaragoza, and J. Blanco, "Solar Desalination," in Annual Review of Heat Transfer, Vol. 15. New York: Begell House, Inc., 2012.

[53] Miller J. E. 2003. Review of Water Resources and Desalination Technologies. Sandia National Laboratories, Albuquerque, NM. 49 pp. Available from http://prod.sandia.gov/techlib/access-control.cgi/2003/030800.pdf. (Accessed May 19, 2017).

[54] K.S. Spiegler and Y.M. El-Sayed, A Desalination Primer, Balaban Desalination Publications, Santa Maria Imbaro, Italy (1994).

[55] How to Design Solar PV System. Available from http://www.leonics.com/support/article2_12j/articles2_12j_en.php. (Accessed March 15, 2017).

[56] Hangzhou Iontech Environmental Technology Company Limited, 2014. Supplier quotations for ion exchange membranes. Hangzhou, China.